Seasonal and diel variations in the vertical distribution, composition, abundance and biomass of zooplankton in a deep Chilean Patagonian fjord

Nur Garcia-Herrera [Corresp., 1, 2] , **Astrid Cornils** [1] , **Jürgen Laudien** [1] , **Barbara Niehoff** [1] , **Juan Höfer** [3, 4, 5] , **Günter Försterra** [3] , **Humberto E González** [4, 6] , **Claudio Richter** [1, 2]

[1] Alfred Wegener Institute, Helmholtz Centre for Polar and Marine Research, Bremerhaven, Germany

[2] University of Bremen, Bremen, Germany

[3] Escuela de Ciencias del Mar, Pontificia Universidad Católica de Valparaíso, Valparaíso, Chile

[4] Research Center: Dynamics of High Latitude Marine Ecosystems (IDEAL), Punta Arenas, Chile

[5] Fundación San Ignacio de Huinay, Huinay, Chile

[6] Institute of Marine and Limnological Sciences, Universidad Austral, Valdivia, Chile

Corresponding Author: Nur Garcia-Herrera
Email address: nur.garcia.herrera@awi.de

Comau Fjord is a stratified Chilean Patagonian fjord characterized by a shallow brackish surface layer and a >400 m layer of aragonite-depleted subsurface waters. Despite the energetic burden of low aragonite saturation levels to calcification, Comau Fjord harbours dense populations of cold-water corals (CWC). While this paradox has been attributed to a rich supply of zooplankton, supporting abundance and biomass data are so far lacking. In this study, we investigated the seasonal and diel changes of the zooplankton community over the entire water column. We used a Nansen net (100 μm mesh) to take stratified vertical hauls between the surface and the bottom (0-50-100-200-300-400-450 m). Samples were scanned with a ZooScan, and abundance, biovolume and biomass were determined for 41 taxa identified on the web-based platform EcoTaxa 2.0. Zooplankton biomass was the highest in summer (209 g dry mass m^{-2}) and the lowest in winter (61 g dry mass m^{-2}). Abundance, however, peaked in spring, suggesting a close correspondence between reproduction and phytoplankton spring blooms (Chl *a* max. 50.86 mg m^{-3}, 3 m depth). Overall, copepods were the most important group of the total zooplankton community, both in abundance (64-81%) and biovolume (20-70%) followed by mysids and chaetognaths (in terms of biovolume and biomass), and nauplii and Appendicularia (in terms of abundance). Throughout the year, diel changes in the vertical distribution of biomass were found with a daytime maximum in the 100-200 m depth layer and a nighttime maximum in surface waters (0-50m), associated with the diel vertical migration of the calanoid copepod family Metridinidae. Diel differences in integrated zooplankton

abundance, biovolume and biomass were probably due to a high zooplankton patchiness driven by biological processes (e.g., diel vertical migration or predation avoidance), and oceanographic processes (estuarine circulation, tidal mixing or water column stratification). Those factors are considered to be the main drivers of the zooplankton vertical distribution in Comau Fjord.

1 # Seasonal and diel variations in the vertical
2 # distribution, composition, abundance and biomass of
3 # zooplankton in a deep Chilean Patagonian fjord

4 Nur Garcia-Herrera[1,2], Astrid Cornils[1], Jürgen Laudien[1], Barbara Niehoff[1], Juan Höfer[3,4,5],
5 Günter Försterra[3], Humberto E. González[4,6], Claudio Richter[1,2]
6
7 [1] Alfred Wegener Institute, Helmholtz Centre for Polar and Marine Research, Bremerhaven,
8 Germany
9 [2] University of Bremen, Germany
10 [3] Escuela de Ciencias del Mar, Pontificia Universidad Católica de Valparaíso, Valparaíso, Chile
11 [4] Research Center: Dynamics of High Latitude Marine Ecosystems (IDEAL), Punta Arenas,
12 Chile
13 [5] Fundación San Ignacio de Huinay, Chile
14 [6] Institute of Marine and Limnological Sciences, Universidad Austral, Valdivia, Chile
15
16 Corresponding author:
17 Nur Garcia-Herrera
18 Am Alten Hafen 26, Bremerhaven, 27568, Germany
19 Email address: nur.garcia.herrera@awi.de
20

Abstract

Comau Fjord is a stratified Chilean Patagonian fjord characterized by a shallow brackish surface layer and a >400 m layer of aragonite-depleted subsurface waters. Despite the energetic burden of low aragonite saturation levels to calcification, Comau Fjord harbors dense populations of cold-water corals (CWC). While this paradox has been attributed to a rich supply of zooplankton, supporting abundance and biomass data are so far lacking. In this study, we investigated the seasonal and diel changes of the zooplankton community over the entire water column. We used a Nansen net (100 μm mesh) to take stratified vertical hauls between the surface and the bottom (0-50-100-200-300-400-450 m). Samples were scanned with a ZooScan, and abundance, biovolume and biomass were determined for 41 taxa identified on the web-based platform EcoTaxa 2.0. Zooplankton biomass was the highest in summer (209 g dry mass m^{-2}) and the lowest in winter (61 g dry mass m^{-2}). Abundance, however, peaked in spring, suggesting a close correspondence between reproduction and phytoplankton spring blooms (Chl *a* max. 50.86 mg m^{-3}, 3 m depth). Overall, copepods were the most important group of the total zooplankton community, both in abundance (64-81%) and biovolume (20-70%) followed by mysids and chaetognaths (in terms of biovolume and biomass), and nauplii and Appendicularia (in terms of abundance). Throughout the year, diel changes in the vertical distribution of biomass were found with a daytime maximum in the 100-200 m depth layer and a nighttime maximum in surface waters (0-50 m), associated with the diel vertical migration of the calanoid copepod family Metridinidae. Diel differences in integrated zooplankton abundance, biovolume and biomass were probably due to a high zooplankton patchiness driven by biological processes (e.g., diel vertical migration or predation avoidance), and oceanographic processes (estuarine circulation, tidal mixing or water column stratification). Those factors are considered to be the main drivers of the zooplankton vertical distribution in Comau Fjord.

Keywords. zooplankton, seasonality, diel vertical migration, cold-water corals (CWC), ZooScan, EcoTaxa, Comau Fjord, Chilean Patagonia.

Introduction

Coastal marine ecosystems are among the most productive on earth (Mann & Lazier, 1991). They provide substantial economic and ecological services, such as high biological production, nutrient cycling or shoreline stability and erosion control (Escribano, Fernández & Aranís, 2003; Liu et al., 2010; Pan et al., 2013; Barbier, 2017). The Chilean fjord region extends over large and complex hydrographic and geomorphologic conditions, particularly rich in productivity and

55   biodiversity (Försterra, Häussermann & Laudien, 2017; Häussermann, Försterra & Laudien,
56   2021), but also endangered by human exploitation, which has been increasing significantly – e.g.
57   salmon aquaculture – over the last two decades (Iriarte, González & Nahuelhual, 2010;
58   Buschmann, Niklitschek & Pereda, 2021; Navedo & Vargas-Chacoff, 2021).

59   The hydrography of the fjords and channels of Patagonia can be considered a transitional
60   estuarine-marine system where a surface layer of silicate-rich terrestrial freshwater meets nitrate-
61   and phosphate-rich marine waters. These fjords receive freshwater from rivers, surface runoff
62   and groundwater flow due to the high rainfall and glacier melting (Pantoja, Iriarte & Daneri,
63   2011). The upper brackish layer within the top 10 m water depth is usually poor in nitrate and
64   phosphate but rich in silicate and organic matter from terrestrial inputs (Sánchez, González &
65   Iriarte, 2011). Below the halocline, a water mass with higher salinity (>31), named Modified
66   Subantarctic Water (MSAAW), flowing landward from the adjacent oceanic area provides the
67   fjords with macronutrients (nitrate and phosphate). Both water masses, surface-freshwater and
68   MSAAW, generate a two-layer structure in the water column with sharp vertical and more
69   gradual horizontal salinity gradients (Sievers & Silva, 2008; Pérez-Santos et al., 2014; Meerhoff
70   et al., 2019). The summer stratification creates a barrier which may hinder the exchange of
71   nutrients within the water column, altering the functioning of the pelagic food web and
72   productivity patterns (Silva, Calvete & Sievers, 1997; González et al., 2011). During austral
73   spring, the Comau Fjord receives an intense riverine input of fresh water, rich in silicic acid used
74   by bloom-generating diatoms and, thus, leading to high primary production (González et al.,
75   2010). In austral summer, the high concentration of phytoplankton promotes an increase in the
76   abundance and biomass of zooplankton as secondary producers (Antezana, 1999; González et al.,
77   2010). In fjord systems, seasonal patterns are modulated by other oceanographic processes, such
78   as estuarine circulation (Palma & Silva, 2004), tidal regimes and lateral advection (Castro et al.,
79   2011) or water column stratification (Sánchez, González & Iriarte, 2011) influencing the
80   zooplankton biomass and community structure on shorter time scales.

81   Zooplankton plays an essential role in the functioning of marine ecosystems and in the oceanic
82   carbon cycle. It includes a wide variety of organisms and displays extreme variability in terms of
83   community composition and vertical, seasonal and geographical distribution (Palma & Kaiser,
84   1993). Many taxa are known to perform diel vertical migrations (DVM), most likely to evade
85   predators (Stich & Lampert, 1981; Iwasa, 1982). According to the predator-evasion hypothesis,
86   migrating zooplankton resides in deep waters during daytime hours where the probability of
87   being perceived by visually orientated predators is lower than if they remained in better
88   illuminated shallow waters, and at night, in the refuge of darkness, they migrate upwards to feed.
89   However, DVM is not performed by all organisms in a zooplankton community or even not by

90   all individuals of one species. For example, while late copepodites and adults of the copepod
91   genus *Metridia* migrate, a large fraction of the young developmental stages remains in surface
92   waters, saving the energy of performing the DVM, suggesting a lower probability of being
93   perceived and consumed by visual predators (Hays, 1995). Both, migrant and non-migrant
94   species are important elements of the biological carbon pump via the production of sinking fecal
95   pellets that transport carbon from surface waters to the seafloor (Urrère & Knauer, 1981; Fowler
96   & Knauer, 1986; Emerson & Roff, 1987). Zooplankton also provides a trophic link between
97   primary production and higher consumers such as fish, birds and mammals, but also invertebrate
98   predators, such as corals (Nemoto, 1970; Gili et al., 2006; Höfer et al., 2018).

99   Cold-water corals (CWC) rely on zooplankton as their principal food source to maintain their
100   physiological processes, such as respiratory metabolism and growth (Carlier et al., 2009; Mayr et
101   al., 2011; Naumann et al., 2011). Therefore, their diet depends on the zooplankton seasonal, diel
102   and vertical distribution. In Comau Fjord, azooxanthellate scleractinian CWC are wide-spread
103   even in deep aragonite-undersaturated waters (Häussermann & Försterra, 2007; Fillinger &
104   Richter, 2013a; Jantzen et al., 2013a). In the latter, the dissolution of exposed parts of the
105   skeleton, enhanced bioerosion, and reduced CWC growth and survival have been observed
106   (McCulloch et al., 2012; Maier et al., 2016). The calcification of the CWC skeleton is
107   energetically costly, and thus food requirements in these adverse environments are higher
108   compared to aragonite-saturated waters (Maier et al., 2016). According to Fillinger & Richter,
109   (2013b), in Comau fjord, the CWC *Desmophyllum dianthus* thrives but coral densities decrease
110   below 280 m despite available substrate, suggesting that lower oxygen and pH concentrations,
111   combined with a shortage of zooplankton could be limiting coral growth. However, up to now
112   little is known about the zooplankton of Comau Fjord in the northern Patagonian region and its
113   role in sustaining the CWC communities living in the fjord. Most studies were carried out in the
114   central-southern part of Patagonia (from Penas Gulf to Cape Horn, S 46.50° – S 55.55°), while
115   studies performed in the northern area (from Puerto Montt to San Rafael Lagoon, S 41.20° – S
116   46.40°) mainly focused on selected microzooplankton taxa in the upper water column, on bulk
117   measurements of zooplankton biomass, or on the carbon flow through the pelagic food web (e.g.
118   Palma, 2008 and references therein; Villenas, Soto & Palma, 2009; González et al., 2010, 2011;
119   Palma et al., 2011; Sánchez, González & Iriarte, 2011). Other studies addressed the physical
120   oceanographic processes and their effect on zooplankton distribution (e.g. Marín & Delgado,
121   2009; Castro et al., 2011) and their relationship with zoo- and ichthyoplankton growth and
122   feeding (Landaeta et al., 2015a,b). Recent studies have investigated zooplankton migration
123   patterns by acoustic backscatter and vertical velocity profiles (Valle-Levinson et al., 2014; Díaz-
124   Astudillo, Cáceres & Landaeta, 2017; Pérez-Santos et al., 2018). The information on

125   zooplankton diversity and migration patterns is, however, still very fragmentary and the linkage

126   between the abundance of CWC and zooplankton supply in Comau Fjord remains unknown.

127   In this study, we aim to describe the diel, vertical, and seasonal distribution of mesozooplankton

128   groups of Comau Fjord, with a focus on the dominating taxa, particularly those that migrate and

129   are more likely to aggregate. Samples were collected at day and night hours with vertical net

130   hauls through the whole water column in spring, summer, autumn and winter. They were

131   processed with a high-resolution image analysis system (ZooScan, Gorsky et al. 2010). The

132   zooplankton taxa were identified using EcoTaxa 2.0 (Picheral, Colin & Irisson, 2017), allowing

133   to assess the influence of seasonal environmental changes on zooplankton dynamics, and the

134   food naturally available to CWC.

135

Materials & Methods

137   Field work was carried out in Comau Fjord, Northern Patagonia, Chile (Fig. 1). Zooplankton was

138   sampled four times at a fixed station (42°14.95S, 72°28.83W) in central Comau Fjord: in austral

139   spring (28th September 2016; three days before spring tide-new moon), summer (17th January

140   2017; two days after spring tide-full moon), autumn (7th May 2017; three days before spring tide-

141   full moon), and winter (29th July 2017; one day before neap tide), during both day (noon) and

142   night (midnight). Samples were collected with a 70 cm-diameter Nansen closing net (mesh size:

143   100 μm) equipped with a non-filtering cod end. Vertical hauls were carried out at 0.45 m s^{-1} to

144   sample the depth strata 0-50-100-200-300-400-450 m. Immediately after the collection, the

145   samples were sieved through a 50 μm mesh and preserved in 4% borax-buffered formaldehyde

146   for laboratory analyses. After every zooplankton haul, a CTD multi-probe (SBE 19plusV2

147   Profiler - with RS 232 Interface, Sea-Bird Electronics Inc.) was deployed from the surface to the

148   bottom, measuring conductivity, temperature, oxygen, pH and chlorophyll *a* (Chl *a*)-

149   fluorescence.

150   In the laboratory, fixed zooplankton samples were washed with fresh water and prepared for

151   analysis with a ZooScan digital imaging system (Grosjean et al., 2004; Gorsky et al., 2010).

152   ZooScan (CNRS patent, www.hydroptic.com) provides a quick and reliable method for the

153   analysis of preserved plankton samples, storing digitized images for later examination,

154   reprocessing and dissemination. Concentrated samples were subsampled with a Folsom plankton

155   splitter to avoid images being cluttered with more than approximately 1000-1500 individuals. Up

156   to six binary splitting steps were carried out (corresponding to a minimum 1/64th fraction of the

157   original sample). Routinely, the two final splits were scanned with ZooScan yielding images of

158   2400-dpi resolution (14200×22700 pixels). The hinged base of the ZooScan allowed the

159   recovery of the complete undamaged subsample, which was later stored in 70% ethanol for

160   archiving. Most overlapping individuals on the scanning surface were manually separated to

161   ensure an even distribution before scanning. Image analysis was performed with the software

162   ZooProcess (Gorsky et al., 2010), a plug-in for the image processing and analysis software

163   ImageJ (Schneider, Rasband & Eliceiri, 2012). The processing involved (1) the automatic

164   subtraction of background noise, (2) the automatic thresholding and detection of objects, and (3)

165   the automated storage of detected objects in separate images ("vignettes"). Below 300 μm,

166   organisms were often too blurred to be identified. Thus, the ZooScan detection limit was set at

167   the standard of 300 μm so that detected zooplankton sizes ranged from 0.3 to 59 mm. The

168   automatic processing of the scans was successful in 75-80% of the cases where vignettes with

169   one individual were obtained. However, despite the manual separation, some individuals

170   overlapped, resulting in vignettes with two or more objects. These objects on the pictures were

171   manually separated using the "separation with mask" tool of the ZooProcess software. Separated

172   vignettes were stored, while the original vignette, containing multiple objects was eliminated

173   from the database to avoid duplicate counts. In some cases, the separation of individuals was not

174   possible as cutting the vignette would mean losing information about the morphology of the

175   organisms (i.e. cutting overlapping urosomes from two different copepods or small copepods

176   embedded in cnidarians). Overall, the contribution of vignettes with multiple objects that could

177   not be separated was always <10% of the total amount of vignettes.

178   Vignettes were subjected to the semi-automated taxonomic classification in EcoTaxa 2.0

179   (Picheral, Colin & Irisson, 2017). This web-based machine learning application uses training sets

180   of expert-identified taxa and random forest classification to automatically identify and sort the

181   objects. Although EcoTaxa contains more than 160 million objects on its server, no ZooScan

182   training set was available for Patagonian waters. Therefore, manual identification of individuals

183   on a subset of the images was first necessary to train an initial model, which was later used by

184   the system to classify the scanned organisms. The initial learning set with Patagonian organisms

185   improved progressively its prediction by sorting more objects into the given categories. This

186   produced the final learning set for the classification of the entire image data set. At the end, all

187   classified objects were individually validated to assure a correct classification. The organisms

188   were classified to the lowest possible taxonomic level; for most copepods this was the family

189   level. However, small calanoid copepods (<1.5 mm) were not distinguishable on family level and

190   were thus comprised as one category: "Calanoids (<1.5 mm)" including five groups (copepodites

191   (all calanoid taxa, <1mm), Clausocalanidae, Microcalanidae, small Calanidae (*Neocalanus* spp.)

192   and Paracalanidae). Developmental stages were included in the corresponding taxon as long as

193   they were clearly identifiable. Only for calanoid copepods, the classification of some
194   developmental stages was not clear and therefore, they were included into the category
195   "copepodites", which included developmental stages of different calanoid copepod taxa. The
196   category Cnidaria was constituted by organisms from the class Hydrozoa (mostly medusa and
197   Siphonophorae). Another category contained all images that were out of focus ("bad focus") and
198   likely comprised individuals from all copepod taxa, in total 6,766 vignettes. From the total of
199   83,516 vignettes, 23,227 could not be assigned to zooplankton taxa, but were labelled as
200   "detritus", "feces", "fiber", "leg" "bubble" and "other" and were not considered in our analyses.
201   ZooProcess provides information about the length and width of each object, allowing the
202   calculation of its volume as a proxy for its biomass (Gorsky et al., 2010). The program
203   automatically fits an ellipse around the object, from which the major and minor axis and volume
204   (V) is computed:

205    $V\ (mm^3) = \frac{4}{3} \times \pi \times \frac{major\ axis\ (mm)}{2} \times \left(\frac{minor\ axis\ (mm)}{2}\right)^2$

206   Biovolume (BV) was then calculated as the sum of the volumes of all objects (ΣV) divided by
207   the fraction of the sample (e.g., F=1/64) and by the volume filtered by the Nansen net (V_N):

208    $BV\ \left(mm^3/m^3\right) = \frac{\left[\frac{\Sigma V\ (mm^3)}{F}\right]}{V_N\ (m^3)}$

209   V_N was calculated as:

210    $V_N\ \left(m^3\right) = \left[\pi \times \left[\frac{net\ diameter\ (m)}{2}\right]^2\right] \times depth\ interval\ (m) \times filtration\ efficiency$

211   where filtration efficiency was assumed as the theoretical 100% efficiency (value = 1).
212   Flowmeter readings were not used because the speed of the net haul was below the measuring
213   range of the mechanical flowmeter.

214   For the estimation of biomass, a regression between the dry mass (DM) of a specimen and its
215   body area [DM (μg) = ($a\ A^b$)] was used (Hernández-León & Montero, 2006; Lehette &
216   Hernández-León, 2009), where A is the area (mm^2) of each scanned individual. The regression
217   required different conversion factors depending on the organism, as for instance, gelatinous
218   zooplankton with high water content may not be compared to crustaceans or echinoderms
219   (Table 1). Such coefficients have been successfully published in previous studies for mid-latitude
220   shelf areas (Marcolin, Gaeta & Lopes, 2015) or the Chilean upwelling region (Tutasi &
221   Escribano, 2020).

222   The biomass (B) of each taxon was then calculated as the sum of the individual dry masses of the
223   respective taxon (ΣDM) divided by the fraction of the sample (e.g., F=1/64) and by the volume
224   filtered by the Nansen net (V_N):

225     $$B\left(mg\ dry\ mass/m^3\right) = \frac{\left[\frac{\Sigma DM(mg)}{F}\right]}{V_N(m^3)}$$

226   Biovolume and biomass were calculated to obtain the sum of the values of all individuals for a
227   given taxon. In multiple vignettes, the automatic calculation of biovolume and biomass was not
228   possible because of overlapping specimens from different taxa. Then, the organisms were
229   counted manually and biovolume and biomass were estimated by multiplying the mean volume
230   or DM of the given taxon from all automatic calculations by the extra number of multiple
231   vignettes. Groups with large size variability (e.g., chaetognaths, cnidarians or Euchaetidae) were
232   divided into two categories, small (0.003-4.242 mm^3) and large (4.243-90.083 mm^3) in order to
233   get a better biovolume/biomass assessment.

234   The integrated values of abundance, biovolume and biomass, were calculated down to 400 m
235   water depth for all seasons, taking out the last 50 m from summer and winter, to make it
236   comparable to the spring and autumn seasons, where samples were collected down to 400 m.

237   The relationships among physicochemical variables and each taxon's abundance were analyzed
238   using a redundancy analysis (RDA). RDA is a constrained ordination procedure which allows the
239   assessment of how much of the variation of one set of response variables (i.e. zooplankton
240   abundances) is explained with another set of variables (i.e. physicochemical variables). The
241   RDA is a multiresponse analysis which summarizes the linear relationships among dependent
242   and independent variables into a matrix followed by a principal component analysis (PCA).
243   Mean values of temperature, salinity, oxygen, and Chl *a* (log transformed) for the entire water
244   column were used as explanatory variables. RDA was performed in R (R Core Team, 2021) by
245   using the *rda* function of the *vegan* package (Oksanen et al., 2019). The problems caused by
246   non-normal distributions in testing the significance of RDA results were solved by a permutation
247   test (10,000 iterations) (Borcard, Gillet & Legendre, 2011) using the *anova.cca* function from the
248   *vegan* package. All abundance data were logarithmically transformed before analysis.

249   The centroid depths (CD) of the zooplankton groups for each sampling event were calculated as:
250   CD = $\sum (p_k \times z_k) / \sum p_k$, where p_k is the number of organisms in the stratum k, and z_k is the mean
251   depth of the stratum k. CD were calculated for abundance and biovolume -not biomass- to better
252   represent the gelatinous zooplankton groups (e.g. Cnidaria). Due to the lack of replication, these
253   values were compared using a contingency table by means of a Chi-square test, in order to test

254   the significance of night-day changes in CD. The Chi-square test compares the critical values to
255   assess their significance according to their degrees of freedom (df) = $(r - 1)(c - 1)$, where r is
256   the number of rows and c the number of columns in the contingency table. After showing
257   significant day-night differences in CD, a dissimilarity analysis (function *simper* from *vegan*
258   package) performed pairwise comparisons of zooplankton taxa and estimated the average
259   contribution of each taxon to the average overall Bray-Curtis dissimilarity. We listed the
260   zooplankton taxa which cumulatively contributed at least to 70% of the night-day differences
261   observed.

262

Results

264   The physicochemical parameters measured throughout the water column of Comau Fjord
265   showed a stronger seasonal variability in surface waters (0-50 m) than in deep waters (50-450 m)
266   (Fig. 2). The temperature profile indicated summer stratification down to 17 m water depth,
267   followed by surface cooling, breakdown of the thermocline in autumn, and reverse temperature
268   gradients in winter and spring. Accordingly, the surface temperature values were the lowest in
269   winter and spring (8.6-11 °C), and the highest in summer (16.7 °C), getting cooler again in
270   autumn (12 °C). In deeper waters, temperatures were more stable with an average value of 11.4 ±
271   0.2 °C (mean ± SD; Fig. 2A). Salinity was between 10-30 in the upper 20 m and 32.9 ± 0.4
272   below 20 m (Fig. 2B). The pH ranged between 8.5 and 7.7 in the upper 50 m and was 7.9 ± 0.1
273   in deeper waters in all seasons, except for autumn, where we interpret the sudden drop of pH
274   values as an instrument malfunction (Fig. 2C). Oxygen concentration showed the largest
275   variations in the upper 50 m during the spring season (137.2-410.5 μmol kg^{-1}), while below 100
276   m depth it was on average 180 ± 9.3 μmol kg^{-1} (Fig. 2D). The chlorophyll *a* (Chl *a*)
277   concentration peaked in early spring (50.86 mg Chl *a* m^{-3} at 3 m depth), followed by a decrease
278   towards the end of the summer and low values through autumn and mid-winter (2.5-5 mg Chl *a*
279   m^{-3} at 5-10 m depth) (Fig. 2E). Below 25 m, the concentration of Chl *a* was <1.8 ± 0.5 mg m^{-3}
280   throughout the year (Fig. 2E).

281   The zooplankton community exhibited large seasonal and diel differences. Abundance,
282   integrated over the upper 400 m of the water column (individuals m^{-2}) showed the highest values
283   in spring and the lowest during autumn for both day and night (Fig. 3A). The integrated
284   biovolume (cm^3 m^{-2}) and biomass (g dry mass m^{-2}) showed a different pattern with the highest
285   values in summer and the lowest in autumn and winter (Fig. 3B, C). Diel differences in
286   integrated abundances generally showed higher values during the day than at night, except for
287   autumn (Fig. 3A). Diel differences in integrated biovolume and biomass were surprisingly large,

288   with generally higher values during the night, except for spring (Fig. 3B, C), indicating that
289   during daytime, particularly in spring, zooplankton was more numerous but smaller in size.

290   Overall, the centroid depth dissimilarity analysis showed that in spring, fewer taxa contributed to
291   the significant day-night differences (Chi-square Pr <2.2 e^{-16}, p <0.001) both in abundance and
292   biovolume, while in summer and autumn the number of contributing zooplankton groups
293   increased (Fig. 4). The zooplankton vertical distribution showed that abundance exhibited the
294   highest values during day and night in the 0-50 m layer at all seasons, with the exception of
295   autumn during day time, where abundances showed low values throughout the water column
296   (Fig. 5A). The lowest abundances were found in >300 m depth in spring, summer and winter,
297   and in 50-100 m depth in autumn during day and night time (Fig. 5A). The highest biovolume
298   and biomass daytime values were observed in 0-50 m and 100-200 m water depth in spring and
299   summer, and in 100-300 m in autumn. However, in winter, daytime biovolume and biomass were
300   similarly low throughout the entire water column (Fig. 5B, C). At night, the highest biovolume
301   and biomass values were found at the surface (0-50 m) in all seasons. The lowest biovolume and
302   biomass values were found in >300 m depth in spring and summer, in 50-100 m and 200-300 m
303   depth in autumn and in >50 m depth in winter (Fig. 5B, C).

304   The taxonomic composition greatly differed when considering biovolume and abundance (Fig. 6,
305   7A; biovolume—not biomass—was used to better represent the gelatinous taxa). Copepoda were
306   generally the dominant group, constituting 20-70% of the total biovolume, and 64-81% of the
307   total abundance. Within the copepod community, individuals smaller than 1.5 mm included (a)
308   copepodites and adults of small calanoid genera, such as Clausocalanidae, Microcalanidae,
309   Neocalanidae and Paracalanidae; (b) cyclopoids of the genera *Oithona* and *Oncaea*; (c)
310   harpacticoids; and (d) nauplii. These small copepods accounted for 58-86% of the total
311   abundance within the copepod community. Overall, 14 out of 41 taxa contributed 45-98% of the
312   total biovolume and 45-86% of the total zooplankton abundance (Fig. 6). The other 27 taxa were
313   constituted by copepods (Acartiidae, Aetideidae, Calanoida (non-identifiable), Candaciidae,
314   Centropagidae, Copepoda (non-identifiable), Eucalanidae, Heterorhabdidae, Lucicutiidae,
315   Oncaeidae, Pontellidae, Rhincalanidae), Actinopterygii (eggs and larvae), Appendicularia,
316   Ascidiacea (larvae), Brachiopoda (larvae), Bryozoa (larvae), Cirripedia (nauplii and cypris),
317   Cladocera, Decapoda (larvae), Echinodermata (larvae), eggs, Isopoda, Nemertea (larvae),
318   Platyhelminthes (larvae), Polychaeta (larvae) and non-identifiable organisms.

319   The contribution of groups other than copepods to the total zooplankton community differed
320   regarding biovolume and abundance. For biovolume, Cnidaria (2-23%) and Mysida (1-21%)
321   constituted a large part of the zooplankton community, followed by Chaetognatha (3-15%).

322   Metanauplii and calyptopis stages of Euphausiacea were found mostly in spring and summer,
323   accounting for 0-7% of the total biovolume. A single adult specimen found during winter in 0-50
324   m water depth at night raised the total biovolume of this taxon to 65%. Regarding abundance,
325   copepod nauplii (2-9%, with their maximum in spring and minimum in autumn) and
326   Appendicularia (0.4-6%) were the second and third most abundant groups after Copepoda,
327   respectively. The fourth most abundant group differed among seasons: Echinodermata larvae
328   (5% in spring), Mollusca larvae (2-5% in summer, 3-9% in autumn), Ostracoda (4-5% in
329   autumn) and Bryozoa larvae (2-10% in winter). Across all samples and seasons, taxa that
330   represented more than 5% of total biovolume were Cnidaria (13%), Calanidae (12.9%), Mysida
331   (12.7%), Metridinidae (12.6%), Chaetognatha (9.6%) and Euchaetidae (8.7%). The most
332   abundant groups with more than 5% of the total abundance were Harpacticoida (14.0%),
333   Cyclopoida (9.1%) and Metridinidae (8.4%) (Fig. 6, 7A).

334   The integrated abundance of small and large copepods and chaetognaths showed the highest
335   abundance in spring and generally low values in autumn and winter (Table 2). Highest
336   abundances of copepod nauplii and cnidarians were found in early spring with a minimum in
337   autumn and raising up again in late-winter. Mysida presented a stable abundance throughout the
338   year with a minimum in summer. These groups clearly presented different vertical distributions
339   (Fig. 7). Metridinidae, a family of large copepods with high biovolume and abundance, resided
340   generally above 200 m, exhibiting a peak between 100-200 m during the day. At night, 74% of
341   their abundance and 77% of their biovolume were found in the upper 50 m (Fig. 7B). On
342   average, larger individuals (0.62 ± 0.3 mm^3; average size $\pm$ SD) were found in 100-200 m waters
343   during the day and night. In spring, a significant proportion of the Metridinidae was found during
344   the day in shallow waters where smaller individuals (0.14 ± 0.08 mm^3) were observed. At
345   nighttime, a fraction of those large and small individuals residing at intermediate waters were
346   found also in shallow waters (Fig. 8A). The Calanidae were found mainly in intermediate waters
347   (100-300 m) during daytime, except in spring, where on average larger individuals (1.37 ± 0.5
348   mm^3) resided (Fig 8B). In spring, small specimens of Calanidae (0.30 ± 0.003 mm^3) were found
349   in shallow waters also during daytime (Fig 8B). At nighttime, half of the population (61% and
350   54% of their abundance and biovolume, respectively) were present in shallow waters. In autumn,
351   however, the whole population stayed between 100-400 m. Despite the low number of Calanidae
352   found at shallow waters, they contributed considerably to the biovolume in these layers (Fig. 6).
353   Euchaetidae showed higher abundance and biovolume in the deep part of the water column
354   during day time (100-450 m), ascending to shallower waters at night (Fig. 7I). Small copepods of
355   the taxa Harpacticoida and Cyclopoida were very abundant, but, as expected, they only
356   represented a small fraction of the total biovolume. Harpacticoida were distributed through the

357   whole water column (Fig. 7D). Cyclopoida were mainly present in the upper 50 m during day

358   and night in all seasons (Fig. 7H). Cnidarians were overall not very abundant, but constituted an

359   important fraction of the biovolume, especially in 200-300 m depth during day in all seasons,

360   and 50-100 m depth during day time in summer and autumn. Their highest abundances were

361   generally found in 0-50 m during day and night, while higher biovolumes were detected in

362   deeper layers 200-450 m (Fig. 7E). Throughout the year, Mysida were mainly present in >200 m

363   depth during the day, accounting for 52-100 % of its abundance and 89-100% of its biovolume.

364   In spring, at night a high proportion of their abundance and biovolume were found in shallow

365   waters while in summer only a fraction of their abundance was found in 0-50 m. In autumn and

366   winter the shallowest depth mysids were found was up to 50 m both during day and night (Fig.

367   7F). Chaetognatha presented the highest abundances in the 0-50 m water depth during day and

368   night in all seasons. Their biovolume, however, peaked at 100-300 m during day and at 0-50 m

369   during night (Fig. 7G).

370   Overall, the four predictor variables (fluorescence (Chl a), oxygen, temperature, salinity)

371   explained 44.3% and 33.69% of the total variation in abundance and biovolume, respectively

372   (Fig. S1). The first axis of the RDA explained 34.15% (abundance) and 25.4% (biovolume) of

373   the total variation while the second axis only accounted for 10.15% (abundance) and 8.29%

374   (biovolume). Relationships between the parameters and the first RDA axis were highest for Chl

375   a, while temperature was related to the second RDA axis. For both abundance and biovolume the

376   main differences were observed between day and night samples in shallow waters (0-50 m),

377   during spring and summer. The abundance and biovolume of the major zooplankton groups were

378   positively influenced by Chl *a* concentration, except for mysids and ostracods, while temperature

379   did not seem to have a strong influence on the majority of the groups, except for the large

380   zooplankton (amphipods, Euphausiacea and euphausiids) (Fig. S1).

381

Discussion

Physicochemical properties and mesozooplankton seasonal dynamics

384   The physicochemical observations in our study are consistent with earlier descriptions from

385   Comau Fjord, a temperate fjord connected to the Pacific Ocean by the Chacao Channel and

386   Ancud Gulf. Comau Fjord has an estuarine circulation and is characterized by a strong

387   pycnocline, where surface waters (0-50 m) present higher variability than the deeper and quasi-

388   homogeneous water layer (Fig. 2). Clear differences were observed in temperature, pH, oxygen

389   and Chl *a* in relation to the season, likely caused by the strong seasonal variability in solar

390   radiation (maximum between spring and summer), precipitation and river discharge (maximum
391   in late autumn and winter) (González et al., 2010).

392   Pronounced seasonality of environmental variables often results in high biological production
393   and are associated to seasonal changes in the holoplankton community (Mauchline, 1998;
394   Balbontín & Bustos, 2005; Aracena et al., 2011), and meroplankton abundance (Ladah et al.,
395   2005; Landaeta & Castro, 2006). In Comau Fjord, a thermal inversion of the surface water (0-50
396   m) in winter is visible (Fig. 2), probably due to heat loss in the surface layer caused by winds and
397   the discharge of cold freshwater from rivers and glaciers (Silva, Calvete & Sievers, 1997). Later
398   in the year, the thermal density stratification stabilizes the water column, triggering spring
399   phytoplankton blooms (Iriarte et al., 2007), which usually follow rain events and thus the input
400   of nutrients. This leads to a strong increase in Chl a (Fig. 2E). As shown by previous studies in
401   the area (Palma & Silva, 2004; Vargas et al., 2008; González et al., 2010), this peak in Chl a was
402   most likely due to blooming chain-forming diatoms. The high phytoplankton biomass is
403   expected to be grazed predominantly by copepods, increasing their biomass and establishing the
404   classical diatom-to-zooplankton food web (Palma & Silva, 2004; Vargas et al., 2008; González
405   et al., 2010). Accordingly, the population dynamics of copepods in this study followed the
406   phytoplankton seasonal cycle, with the highest abundance in spring, associated with the
407   maximum concentration in phytoplankton (Table 2). At this time, copepod nauplii and young
408   stages of calanoid copepods, which are indicative of intense zooplankton reproduction,
409   accounted for a large proportion of the zooplankton community. Considering that copepods are
410   the main food source for cnidarians and chaetognaths (Palma & Kaiser, 1993), the higher
411   abundance of carnivorous zooplankton occurring in spring (Table 2) can be attributed to the large
412   copepod abundance at this time of the year. In summer, biovolume and biomass reached their
413   maxima (Fig. 3), which together with a lower abundance, suggests the presence of larger
414   individuals or different groups including species with larger individuals. Subsequently, in
415   autumn and winter, zooplankton abundance, biovolume and biomass decreased. At this time,
416   primary production should be low, as reflected by low Chl a values (Fig. 2E), and likely
417   zooplankton growth was limited by food availability (Escribano et al., 2007). The overall decline
418   in copepod abundance from spring to winter may be explained by the decrease in phytoplankton
419   occurrence and the increasing predation pressure exerted by carnivorous zooplankton. In winter,
420   the plankton in the fjord typically shifts towards a microbial loop based community grazed by
421   heterotrophic nanoflagellates, which become the main mesozooplankton prey (Vargas et al.,
422   2008; González et al., 2010) however, this does not support a high secondary production.

423   The northern part of the Chilean fjord region, the area between Puerto Montt and Guafo Mouth,
424   represents the most productive area of Patagonia in terms of primary production and zooplankton

425 biomass (Palma, 2008). In contrast, the phytoplankton production in the southern area is low due
426 to the stronger influence of glaciers, resulting in cold, fresh and turbid waters (Palma & Rosales,
427 1997; Palma & Silva, 2004; Iriarte et al., 2007; Palma, 2008), and consequently low zooplankton
428 survival and growth (Giesecke et al., 2019). Previous studies described ranges for zooplankton
429 biovolume, expressed as the plankton wet volume, of 65 to more than 1386 ml zooplankton 1000
430 m^{-3} outside Comau Fjord, in the Inner Sea off Chiloé island (Palma, 2008). This is in line with
431 the present results (250-1500 ml zooplankton 1000 m^{-3}), showing an especially high biovolume
432 during summer. Palma & Rosales (1997) also found the highest values of zooplankton
433 biovolume in the northern part (interior of Reloncaví Fjord and Ancud Gulf) with values that
434 ranged between 56 and 1626 ml zooplankton 1000 m^{-3}, but a low zooplankton biovolume in the
435 inner of Comau Fjord. The observed variations may potentially be due to (a) interannual
436 differences with a much lower Chl *a* concentration during the same season of their year of study
437 (Ramírez, 1995); and/or (b) methodological and analytical differences, e.g. different sampling
438 gears and proxies for biomass estimation (i.e. measurement of zooplankton wet volume vs.
439 image analysis in this study). Moreover, the vertical hauls used in this study may most likely
440 underestimate the abundance of very motile organisms able to avoid the net, such as adult
441 euphausiids, megalopae of *Munida gregaria* or large fish larvae, which are also important in
442 terms of density and biomass across west Patagonia (Antezana, 1999).

443 In fjord systems, oceanographic processes such as estuarine circulation, tidal mixing or water
444 column stratification may influence the composition and abundance of zooplankton communities
445 (Palma & Silva, 2004; Sánchez, González & Iriarte, 2011). Overall, copepods were the main
446 contributors to the total biomass and biovolume of the zooplankton community, especially
447 during summer (69-78%). This is in agreement with previous studies showing that in Chilean
448 fjords, planktonic crustaceans, such as copepods and euphausiids, have the highest abundances
449 and biomasses, followed by chaetognaths and gelatinous plankton (Defren-Janson, Schnack-
450 Schiel & Richter, 1999; Palma & Silva, 2004). Copepods are the most abundant and diverse
451 component of marine zooplankton worldwide (Mauchline, 1998), and the abundance of small
452 copepods (<1.5 mm) generally surpasses the abundance of larger ones (Fransz, 1988; Gallienne
453 & Robins, 1998; Gallienne, Robins & Woodd-Walker, 2001). Similarly, small copepods
454 accounted for 58-86% of the total copepod community in the present study. Another important
455 contributor to zooplankton communities in Chilean fjords is the euphausiid *Euphausia vallentini.*
456 The present study revealed young stages of euphausiids during spring and summer but only one
457 adult specimen in winter, indicating that euphausiids are present in Comau fjord, but were not
458 caught efficiently in our samples. This is likely related to the small volume filtered by our net,
459 the patchy distribution of *E. vallentini*, and their ability of avoiding slow nets (Brinton, 1962).

460 Like euphausiids, mysids can form dense swarms, making them a potential food resource for a
461 wide range of organisms, from predatory fishes to benthic CWC. Despite their important
462 contribution to the total zooplankton biovolume in deep waters (Fig. 6), poor attention has been
463 given to their presence in Chilean Patagonia. To our knowledge, there are only two studies
464 describing mysids in this area: Guglielmo & Ianora (1997) found that the most abundant species
465 for the Strait of Magellan is the deep-dwelling *Boreomysis rostrata*; Díaz-Astudillo, Cáceres &
466 Landaeta (2017) found higher abundances of mysids during night and inside the Reloncaví Fjord
467 and Gulf of Ancud. Thus, this study constitutes the first record of mysids in Comau Fjord.

468 ***Zooplankton diel vertical distribution and migration***

469 Biological processes (e.g. diel vertical migration, predator avoidance, location of food patches
470 and mating), together with oceanographic processes (e.g. estuarine circulation or water column
471 stratification) are mechanisms by which the underlying zooplankton behavior present high
472 spatial heterogeneity (Folt & Burns, 1999). In the present study, zooplankton abundance,
473 biovolume and biomass significantly differed between day and night. These differences were
474 probably due to the high patchiness and the vertical distribution the zooplankton exhibited during
475 day and night, especially by larger zooplankton individuals, those able to form swarms (i.e.
476 mysids and euphausiids) and migrate (Fig. 7B-I). For instance, Euchaetidae, Euphausiacea,
477 Metridinidae and Mysida, four of the larger and most important zooplankton groups, changed
478 their centroid depth between day and night contributing to 30-40% of the difference in
479 abundance and 30-38% in biovolume (Fig. 4). To a lesser extent, small organisms, e.g.
480 Appendicularia, Clausocalanidae and Copepoda (nauplii) also contributed to the day-night
481 differences, especially in summer and autumn, however, their contribution was lower (0-29%) in
482 comparison to larger zooplankton organisms.

483 Diel Vertical Migration (DVM) is usually associated with differences in light intensity within the
484 photic zone, taking place periodically in 24 h cycles (Brierley, 2014). During daytime,
485 zooplankton organisms migrate to deeper, darker waters to avoid visual predators, such as fishes,
486 while they come to the surface for feeding at night (Hays, Webb & Frears, 1998). In Comau
487 Fjord, DVM seemed to be related to the size of the zooplankton. Here, large zooplankton taxa,
488 particularly large copepods, that inhabited the intermediate waters (100-300 m) during daytime
489 ascended to shallow waters at night while small organisms, mainly of cyclopoids and
490 harpacticoids, did not perform a clear DVM (Fig. 7B-I). Throughout the year, Cyclopoida
491 centroid depth fluctuated between 40-85 m water depth and Harpacticoida between 149-254 m
492 water depth. These two copepod groups, however, differed with regard to their vertical

493 distribution. The highest abundances of cyclopoid copepods were mainly found in the upper 50

494 m, whereas harpacticoids were found throughout the water column (Fig. 7D).

495 Large individuals from several calanoid copepod taxa (Metridinidae, Calanidae, Euchaetidae),

496 mysids, chaetognaths and cnidarians did perform DVM over 300 m. This agrees with the

497 findings by Hays (1995) that DVM is pronounced in large and pigmented species due to their

498 susceptibility of being perceived by visually orientated predators. Similarly, studies in northern

499 Patagonia have shown that conspicuous zooplankton organisms tend to avoid well illuminated

500 waters (Villenas, Soto & Palma, 2009). According to Hays, Kennedy & Frost (2001), large

501 individuals of *Metridia* usually reside in deep waters, and only a fraction of these ascends to

502 shallow waters at night, whereas smaller individuals stay at the surface continuously. In Comau

503 Fjord, Metridinidae showed the highest values of biovolume and abundance at intermediate

504 depths (100-200 m) during daytime, but in the surface layer (0-50 m) at night, indicating that

505 77% of the entire population migrated towards the surface (Fig 7B). In spring, a proportion of the

506 Metridinidae population was found in shallow waters during the day. This was due to the smaller

507 size of the individuals (Fig. 8A) and the higher amount of food available here. Following the

508 same pattern as Metridinidae, larger individuals of Calanidae were found in deeper waters during

509 daytime, whereas small specimens were found in shallow waters also during daytime in spring,

510 where they may not be hunted by visual predators due to their small size. It is possible that those

511 small organisms were individuals of earlier life stages (i.e. small) or species with a smaller size.

512 Euchaetidae also performed DVM where most of the organisms lived continuously in deep

513 waters (100-450 m) during the day, but a big proportion of the population (60% and 53% of their

514 abundance and biovolume, respectively) migrated to the surface during night, except in winter

515 (Fig. 7I).

516 Mysids accounted for a big proportion (up to 70%) of the total zooplankton biovolume,

517 especially in spring and winter (Fig. 6). During day, they were generally detected in deep waters

518 (>200 m water depth) and at night they migrated upwards, although their DVM pattern were

519 clear only in spring and summer. At night in spring, both abundance and biovolume were high in

520 the 0-50 m water depth whereas in summer only a high abundance was detected at that water

521 depth. The fact that biovolume peaked at 200-300 m in summer at night suggested that only

522 small individuals migrated to shallow waters while larger ones stayed at deeper waters (Fig 7F).

523 Chaetognaths were distributed throughout the water column with the highest biovolumes

524 between 100-300 m, during both day and night (Fig. 7G). This is in accordance with the

525 distribution found by Guglielmo & Ianora (1995) for the Strait of Magellan. A particularly high

526 abundance of chaetognaths in the upper 0-50 m during both day and night and a high biovolume

527 only at night indicated that bigger individuals migrated to shallow waters at night likely to feed
528 on other organisms. South of Comau Fjord, between Boca del Guafo and the Pulluche Channel,
529 the vertical distribution of cnidarians (i.e. Hydromedusae and Siphonophorae) showed highest
530 abundances in the upper 100 m, specifically in the 20-50 m stratum (Palma, Apablaza & Soto,
531 2007). In this study, cnidarian highest abundances were found in 0-50 m during day and night.
532 However, biovolume peaked in every season, except for summer, at 200-300 m, indicating that
533 bigger individuals of cnidarians stayed at deeper waters while small individuals resided in
534 shallow waters.

535 In the 50-100 m water layer a minimum in zooplankton abundance and biomass was found in all
536 seasons (Fig. 5). This "zooplankton gap" could be related to a high concentration of predators in
537 this water depth. In northern Chilean fjords, the high biomasses and abundances of gelatinous
538 organisms are correlated to a decrease in chitinous biomass of other organisms (Palma & Silva,
539 2004; Villenas, Soto & Palma, 2009). It is known that chaetognaths and cnidarians can grow at
540 fast rates, forming dense aggregations that seasonally dominate the zooplankton biomass
541 (Casanova, 1999; Brodeur, Sugisaki & Hunt Jr, 2002) by feeding voraciously on copepods and
542 larvae from other organisms (Lie et al., 1983; Palma & Rosales, 1997). In our study, biovolume
543 of carnivorous organisms ranged between 18 and 83% of the total zooplankton in this water
544 layer, reaching particularly high values in summer and autumn (50-83%) (Fig. 9). These previous
545 evidences suggest that carnivorous organisms may have reduced zooplankton abundance in this
546 depth stratum and predation may play a role in structuring the vertical zooplankton community in
547 Comau Fjord.

548 Mesozooplankton plays an important role in the food web as a food source for many pelagic and
549 benthic organisms (González et al., 2013), including CWC (Gili et al., 2006; Carlier et al., 2009;
550 Mayr et al., 2011). Due to the difficulty of studying CWC *in situ*, little is known about their
551 natural diet and its availability. In Comau Fjord, CWC thrive also in deeper, naturally acidified
552 waters (Häussermann & Försterra, 2007; Försterra, Häussermann & Laudien, 2017). Although
553 the environment is unfavorable, this might be due to the high ingestion rate (e.g. of the CWC
554 *Desmophyllum dianthus*) which showed a positive impact on their calcification rates, regardless
555 of the seawater pH (Martínez-Dios et al., 2020). Zooplankton abundance and biomass are highly
556 influenced by seasonality. Therefore, CWC must be adapted to differences in food availability,
557 i.e. high zooplankton abundances during spring and summer and low concentrations during
558 autumn and winter. Indeed high growth rates of *D. dianthus* were found in summer (Jantzen et
559 al., 2013b) which may be associated with higher zooplankton availability. In winter, when
560 zooplankton biomass is low, CWC may slow down their metabolism to cope with the lower food
561 availability (Naumann et al., 2011). Only recently, a study confirmed that *D. dianthus* preyed on

562 medium and large sized calanoid copepods and euphausiids (Höfer et al., 2018). Based on the
563 present DVM data, shallow-dwelling CWC in Comau Fjord might feed on small copepods (e.g.
564 cyclopoid and calanoid) during the day, and on larger organisms during night hours when
565 zooplankton migrates upwards. Deeper-dwelling corals, by contrast, may mainly encounter
566 larger prey, such as mysids or large calanoid copepods (Calanidae, Euchaetidae) and thus may
567 gain enough energy to upregulate their internal pH in an acidified environment.

568

569 Conclusions

570 The seasonal changes of zooplankton over the entire water column showed that abundance
571 peaked in spring, likely due to spring phytoplankton blooms. In summer, biovolume and biomass
572 were the highest and decreased thereafter over time, reaching the lowest values in late autumn
573 and mid-winter. The low concentration of Chl-*a* during the cold season suggests that primary
574 production was insufficient to support high levels of secondary production. The vertical
575 distribution of zooplankton biovolume and biomass differed between day and night, with a
576 daytime maximum in the 100-200 m water depth and a nighttime maximum in surface waters (0-
577 50 m) associated with the diel vertical migration of the calanoid copepod Metridinidae. Overall,
578 copepods were the dominant group of the total zooplankton community with an important
579 contribution of small organisms (individuals <1.5 mm), followed by mysids, chaetognaths and
580 cnidarians (biovolume and biomass), and nauplii and Appendicularia (abundance). The
581 integrated abundance, biovolume and biomass also showed significant differences between
582 daytime and nighttime values. These differences were probably due to the high zooplankton
583 patchiness driven by both biological and oceanographic processes. Diel vertical migration,
584 predation avoidance, location of food patches as well as estuarine circulation, tidal mixing or
585 water column stratification are considered to be the main drivers of the zooplankton distribution
586 in Comau Fjord.

587

588 Acknowledgements

589 We thank the team of PACOC who contributed to the success of the project. Support during
590 sampling was provided by the scientific and logistic staff from the Fundación San Ignacio del
591 Huinay. Henning Schröder and Manding Suwareh assisted with the sample collection. Thomas
592 Heran, Simon Schöbinger and Jasmin Stimpfle helped with the treatment, analysis and scanning
593 of the samples. Gertraud Schmidt-Grieb provided support in an early phase of the project.

594

References

Antezana T. 1999. Plankton of Southern Chilean fjords: trends and linkages. *Scientia Marina* 63:69–80. DOI: 10.3989/scimar.1999.63s169.

Aracena C, Lange CB, Iriarte JL, Rebolledo L, Pantoja S. 2011. Latitudinal patterns of export production recorded in surface sediments of the Chilean Patagonian fjords (41-55°S) as a response to water column productivity. *Continental Shelf Research* 31:340–355. DOI: 10.1016/j.csr.2010.08.008.

Balbontín F, Bustos C. 2005. Variabilidad en la Composición y Abundancia del Ictioplancton de Chile Austral, durante Noviembre de 2005: Efectos de la Estratificación de la Columna de Agua. In: *Resúmenes Resultados Crucero Cimar -Fiordo 2*. 123–132.

Barbier EB. 2017. Marine ecosystem services. *Current Biology* 27:R507–R510. DOI: 10.1016/j.cub.2017.03.020.

Borcard D, Gillet F, Legendre P. 2011. Canonical Ordination. In: Borcard D, Gillet F, Legendre P eds. *Numerical Ecology with R*. Springer, New York, 153–226.

Brierley AS. 2014. Diel vertical migration. *Current Biology* 24:R1074–R1076. DOI: 10.1016/j.cub.2014.08.054.

Brinton E. 1962. Variable factors affecting the apparent range and estimated concentration of euphausiids in the North Pacific. *Pacific Science* 16:374–408.

Brodeur RD, Sugisaki H, Hunt Jr GL. 2002. Increases in jellyfish biomass in the Bering Sea: Implications for the ecosystem. *Marine Ecology Progress Series* 233:89–103. DOI: 10.3354/meps233089.

Buschmann AH, Niklitschek EJ, Pereda S. 2021. Acuicultura y sus impactos en la conservación de la Patagonia chilena. In: Castilla JC, Armesto JJ, Martínez-Harms MJ eds. *Conservación en la Patagonia chilena: evaluación del conocimiento, oportunidades y desafíos*. Santiago, Chile: Ediciones Universidad Católica de Chile, 367–387.

Carlier A, Le Guilloux E, Olu K, Sarrazin J, Mastrototaro F, Taviani M, Clavier J. 2009. Trophic relationships in a deep mediterranean cold-water coral bank (Santa Maria di Leuca, Ionian sea). *Marine Ecology Progress Series* 397:125–137. DOI: 10.3354/meps08361.

Casanova JP. 1999. Chaetognatha. In: Boltovskoy D ed. *South Atlantic Zooplankton*. Backuys Publ., Leiden, 1353–1374.

Castro LR, Cáceres MA, Silva N, Muñoz MI, León R, Landaeta MF, Soto-Mendoza S. 2011. Short-term variations in mesozooplankton, ichthyoplankton, and nutrients associated with semi-diurnal tides in a patagonian Gulf. *Continental Shelf Research* 31:282–292. DOI: 10.1016/j.csr.2010.09.005.

Defren-Janson K, Schnack-Schiel SB, Richter C. 1999. Mesozooplankton communities in the Magellan region. *Scientia Marina* 63:43–50. DOI: 10.3989/scimar.1999.63s143.

Díaz-Astudillo M, Cáceres MA, Landaeta MF. 2017. Zooplankton structure and vertical migration: Using acoustics and biomass to compare stratified and mixed fjord systems. *Continental Shelf Research* 148:208–218. DOI: 10.1016/j.csr.2017.09.004.

Emerson CW, Roff JC. 1987. Implications of fecal pellet size and zooplankton behaviour to estimates of pelagic-benthic carbon flux. *Marine Ecology Progress Series* 35:251–257. DOI: 10.3354/meps035251.

Escribano R, Fernández M, Aranís A. 2003. Physical-chemical processes and patterns of

638   diversity of the chilean eastern boundary pelagic and benthic marine ecosystems: An
639   overview. *Gayana* 67:190–205. DOI: 10.4067/s0717-65382003000200008.
640 Escribano R, Hidalgo P, González H, Giesecke R, Riquelme-Bugueño R, Manríquez K. 2007.
641   Seasonal and inter-annual variation of mesozooplankton in the coastal upwelling zone off
642   central-southern Chile. *Progress in Oceanography* 75:470–485. DOI:
643   10.1016/j.pocean.2007.08.027.
644 Fillinger L, Richter C. 2013a. Vertical and horizontal distribution of *Desmophyllum dianthus* in
645   Comau Fjord, Chile: a cold-water coral thriving at low pH. *PeerJ*:1–22. DOI:
646   10.7717/peerj.194.
647 Fillinger L, Richter C. 2013b. Abundance of *Desmophyllum dianthus* during expedition
648   Comau2012. In: Alfred Wegener Institute, Helmholtz Centre for Polar and Marine
649   Research, Bremerhaven, PANGAEA,. DOI: https://doi.org/10.1594/PANGAEA.811898.
650 Folt C, Burns C. 1999. Biological drivers of zooplankton patchiness. *Trends in Ecology and*
651   *Evolution* 14:300–305. DOI: 10.1016/S0169-5347(99)01616-X.
652 Försterra G, Häussermann V, Laudien J. 2017. Animal forests in the Chilean Fjords; discoveries,
653   perspectives, and threats in shallow and deep waters. In: Rossi S, Bramanti L, Gori A,
654   Orejas C eds. *Marine Animal Forests*. Springer, Cham,. DOI: http://doi-org-
655   443.webvpn.fjmu.edu.cn/10.1007/978-3-319-21012-4_3.
656 Fowler SW, Knauer GA. 1986. Role of large particles in the transport of elements and organic
657   compounds through the oceanic water column. *Progress in Oceanography* 16:147–194.
658   DOI: https://doi.org/10.1016/0079-6611(86)90032-7.
659 Fransz HG. 1988. Vernal abundance, structure and development of epipelagic copepod
660   populations of the eastern Weddell Sea (Antarctica). *Polar Biology* 9:107–114. DOI:
661   10.1007/BF00442037.
662 Gallienne CP, Robins DB. 1998. Trans-oceanic characterization of zooplankton community size
663   structure using an optical plankton counter. *Fisheries Oceanography* 7:147–158.
664 Gallienne CP, Robins DB, Woodd-Walker RS. 2001. Abundance, distribution and size structure
665   of zooplankton along a 20° west meridional transect of the northeast Atlantic Ocean in July.
666   *Deep-Sea Research II* 48:925–949. DOI: 10.1016/S0967-0645(00)00114-4.
667 Giesecke R, Höfer J, Vallejos T, González HE. 2019. Death in southern Patagonian fjords:
668   copepod community structure and mortality in land- and marine-terminating glacier-fjord
669   systems. *Progress in Oceanography* 174:162–172. DOI: 10.1016/j.pocean.2018.10.011.
670 Gili JM, Rossi S, Pagès F, Orejas C, Teixidó N, López-González PJ, Arntz WE. 2006. A new
671   trophic link between the pelagic and benthic systems on the Antarctic shelf. *Marine Ecology*
672   *Progress Series* 322:43–49. DOI: 10.3354/meps322043.
673 González HE, Calderón MJ, Castro L, Clement A, Cuevas LA, Daneri G, Iriarte JL, Lizárraga L,
674   Martínez R, Menschel E, Silva N, Carrasco C, Valenzuela C, Vargas CA, Molinet C. 2010.
675   Primary production and plankton dynamics in the Reloncaví Fjord and the Interior Sea of
676   Chiloé, Northern Patagonia, Chile. *Marine Ecology Progress Series* 402:13–30. DOI:
677   10.3354/meps08360.
678 González HE, Castro LR, Daneri G, Iriarte JL, Silva N, Tapia F, Teca E, Vargas CA. 2013.
679   Land-ocean gradient in haline stratification and its effects on plankton dynamics and trophic
680   carbon fluxes in Chilean Patagonian fjords (47-50°S). *Progress in Oceanography* 119:32–
681   47. DOI: 10.1016/j.pocean.2013.06.003.
682 González HE, Castro L, Daneri G, Iriarte JL, Silva N, Vargas CA, Giesecke R, Sánchez N. 2011.
683   Seasonal plankton variability in Chilean Patagonia fjords: Carbon flow through the pelagic

684   food web of Aysen Fjord and plankton dynamics in the Moraleda Channel basin.
685   *Continental Shelf Research* 31:225–243. DOI: 10.1016/j.csr.2010.08.010.
686 Gorsky G, Ohman MD, Picheral M, Gasparini S, Stemmann L, Romagnan JB, Cawood A,
687   Pesant S, García-Comas C, Prejger F. 2010. Digital zooplankton image analysis using the
688   ZooScan integrated system. *Journal of Plankton Research* 32:285–303. DOI:
689   10.1093/plankt/fbp124.
690 Grosjean P, Picheral M, Warembourg C, Gorsky G. 2004. Enumeration, measurement, and
691   identification of net zooplankton samples using the ZOOSCAN digital imaging system.
692   *ICES Journal of Marine Science* 61:518–525. DOI: 10.1016/j.icesjms.2004.03.012.
693 Guglielmo L, Ianora A (eds.). 1995. *Atlas of Marine Zooplankton. Straits of Magellan.*
694   *Copepods*. Springer-Verlag, Berlin Heiderlberg. DOI: 10.1007/978-3-642-79139-0.
695 Guglielmo L, Ianora A (eds.). 1997. *Atlas of Marine Zooplankton. Strait of Magellan.*
696   *Amphipods, Euphausiids, Mysids, Ostracods, and Chaetognaths*. Springer-Verlag Berlin
697   Heidelberg. DOI: 10.1007/978-3-642-60340-2.
698 Häussermann V, Försterra G. 2007. Large assemblages of cold-water corals in Chile: a summary
699   of recent findings and potential impacts. *Bulletin of Marine Science* 81:195–207.
700 Häussermann V, Försterra G, Laudien J. 2021. Macrobentos de fondos duros de la Patagonia
701   Chilena: Énfasis en la conservación de bosques sublitorales de invertebrados y algas (Hard
702   bottom marobenthos of Chilean Patagonia: emphasis on conservation of sublitoral
703   invertebrate algal forests). In: Castilla JC, Armesto JJ, Martínez-Harms MJ eds.
704   *Conservación en la Patagonia chilena: evaluación del conocimiento, oportunidades y*
705   *desafíos*. Santiago, Chile: Ediciones Universidad Católica de Chile, 321–344.
706 Hays GC. 1995. Ontogenetic and seasonal variation in the diel vertical migration of the copepods
707   *Metridia lucens* and *Metridia longa*. *Limnology and Oceanography* 40:1461–1465.
708 Hays GC, Kennedy H, Frost BW. 2001. Individual variability in diel vertical migration of a
709   marine copepod: Why some individuals remain at depth when others migrate. *Limnology*
710   *and Oceanography* 46:2050–2054. DOI: 10.4319/lo.2001.46.8.2050.
711 Hays GC, Webb PI, Frears SL. 1998. Diel changes in the carbon and nitrogen content of the
712   copepod *Metridia lucens*. *Journal of Plankton Research* 20:727–737. DOI:
713   10.1093/plankt/20.4.727.
714 Hernández-León S, Montero I. 2006. Zooplankton biomass estimated from digitalized images in
715   Antarctic waters: A calibration exercise. *Journal of Geophysical Research* 111:1–6. DOI:
716   10.1029/2005JC002887.
717 Höfer J, González HE, Laudien J, Schmidt GM, Häussermann V, Richter C. 2018. All you can
718   eat: the functional response of the cold-water coral *Desmophyllum dianthus* feeding on krill
719   and copepods. *PeerJ*. DOI: 10.7717/peerj.5872.
720 Iriarte JL, González HE, Liu KK, Rivas C, Valenzuela C. 2007. Spatial and temporal variability
721   of chlorophyll and primary productivity in surface waters of southern Chile (41.5-43° S).
722   *Estuarine, Coastal and Shelf Science* 74:471–480. DOI: 10.1016/j.ecss.2007.05.015.
723 Iriarte JL, González HE, Nahuelhual L. 2010. Patagonian fjord ecosystems in Southern Chile as
724   a highly vulnerable region: problems and needs. *Ambio* 39:463–466. DOI: 10.1007/s13280-
725   010-0049-9.
726 Iwasa Y. 1982. Vertical migration of zooplankton : a game between predator and prey. *The*
727   *American Naturalist* 120:171–180.
728 Jantzen C, Häussermann V, Försterra G, Laudien J, Ardelan M, Maier S, Richter C. 2013a.
729   Occurrence of a cold-water coral along natural pH gradients (Patagonia, Chile). *Marine*

730 *Biology* 160:2597–2607. DOI: 10.1007/s00227-013-2254-0.

731 Jantzen C, Laudien J, Sokol S, Försterra G, Häussermann V, Kupprat F, Richter C. 2013b. In situ
732   short-term growth rates of a cold-water coral. *Marine and Freshwater Research* 64:631–
733   641. DOI: 10.1071/MF12200.

734 Ladah LB, Tapia FJ, Pineda J, López M. 2005. Spatially heterogeneous, synchronous settlement
735   of *Chthamalus* spp. larvae in northern Baja California. *Marine Ecology Progress Series*
736   302:177–185.

737 Landaeta MF, Bustos CA, Contreras JE, Salas-Berríos F, Palacios-Fuentes P, Alvarado-Niño M,
738   Letelier J, Balbontín F. 2015a. Larval fish feeding ecology, growth and mortality from two
739   basins with contrasting environmental conditions of an inner sea of northern Patagonia,
740   Chile. *Marine Environmental Research* 106:19–29. DOI: 10.1016/j.marenvres.2015.03.003.

741 Landaeta MF, Castro LR. 2006. Larval distribution and growth of the rockfish, *Sebastes capensis*
742   (Sebastidae, Pisces), in the fjords of southern Chile. *ICES Journal of Marine Science*:714–
743   724.

744 Landaeta MF, Contreras JE, Bustos CA, Pérez-Matus A. 2015b. Growth and condition of larval
745   rockfish in a Patagonian fjord-type inlet: role of hydrographic conditions and food
746   availability. *Aquatic Ecology* 49:573–584. DOI: 10.1007/s10452-015-9547-y.

747 Lehette P, Hernández-León S. 2009. Zooplankton biomass estimation from digitized images: a
748   comparison between subtropical and Antarctic organisms. *Limnology and Oceanography:*
749   *Methods* 7:304–308. DOI: 10.4319/lom.2009.7.304.

750 Lie U, Magnesen T, Tunberg B, Aksnes D. 1983. Preliminary studies on the vertical distribution
751   of size-fractions in the zooplankton community in Lindås- Pollene, Western Norway. *Sarsia*
752   68:65–80. DOI: 10.1080/00364827.1983.10420558.

753 Liu KK, Atkinson L, Quinones R, Talaue-McManus L. 2010. *Carbon and nutrient fluxes in*
754   *continental margins*. Springer-Verlag Berlin Heidelberg. DOI: 10.1007/978-3-540-92735-8.

755 Maier C, Popp P, Sollfrank N, Weinbauer MG, Wild C, Gattuso JP. 2016. Effects of elevated
756   pCO2 and feeding on net calcification and energy budget of the Mediterranean cold-water
757   coral *Madrepora oculata*. *Journal of Experimental Biology* 219:3208–3217. DOI:
758   10.1242/jeb.127159.

759 Mann KH, Lazier JRN. 1991. *Dynamics of marine ecosystems: biological-physical interactions*
760   *in the oceans*. Oxford, Blackwell Scientific Publications.

761 Marcolin C da R, Gaeta S, Lopes RM. 2015. Seasonal and interannual variability of zooplankton
762   vertical distribution and biomass size spectra off Ubatuba , Brazil. *Journal of Plankton*
763   *Research* 37:808–819. DOI: 10.1093/plankt/fbv035.

764 Marín VH, Delgado LE. 2009. Diversidad y distribución espacial de copépodos superficiales (0-
765   10 metros) en la zona costera del mar interior de Chiloé (Cimar 10 Fiordos). *Ciencia y*
766   *Tecnología del Mar* 32:95–100.

767 Martínez-Dios A, Pelejero C, López-Sanz À, Sherrell RM, Ko S, Häussermann V, Försterra G,
768   Calvo E. 2020. Effects of low pH and feeding on calcification rates of the cold-water coral
769   *Desmophyllum dianthus*. *PeerJ*. DOI: 10.7717/peerj.8236.

770 Mauchline J. 1998. The biology of calanoid copepods. *Advances in Marine Biology* 33:1–710.

771 Mayr CC, Försterra G, Häussermann V, Wunderlich A, Grau J, Zieringer M, Altenbach A V.
772   2011. Stable isotope variability in a Chilean fjord food web: implications for N- and C-
773   cycles. *Marine Ecology Progress Series* 428:89–104. DOI: 10.3354/meps09015.

774 McCulloch M, Trotter J, Montagna P, Falter J, Dunbar R, Freiwald A, Försterra G, López Correa
775   M, Maier C, Rüggeberg A, Taviani M. 2012. Resilience of cold-water scleractinian corals to

776   ocean acidification: boron isotopic systematics of pH and saturation state up-regulation.
777   *Geochimica et Cosmochimica Acta* 87:21–34. DOI: 10.1016/j.gca.2012.03.027.
778 Meerhoff E, Castro LR, Tapia FJ, Pérez-Santos I. 2019. Hydrographic and biological impacts of
779   a Glacial Lake Outburst Flood (GLOF) in a Patagonian Fjord. *Estuaries and Coasts*
780   42:132–143. DOI: 10.1007/s12237-018-0449-9.
781 Naumann MS, Orejas C, Wild C, Ferrier-Pagès C. 2011. First evidence for zooplankton feeding
782   sustaining key physiological processes in a scleractinian cold-water coral. *Journal of*
783   *Experimental Biology* 214:3570–3576. DOI: 10.1242/jeb.061390.
784 Navedo JG, Vargas-Chacoff L. 2021. Salmon aquaculture threatens Patagonia. *Science* 372:695–
785   696. DOI: 10.1126/science.abj0016.
786 Nemoto T. 1970. Feeding pattern of baleen whales in the ocean. In: Steele JH ed. *Marine food*
787   *chains*. University of California Press, 551.
788 Oksanen J, Blanchet FG, Friendly M, Kindt R, Legendre P, McGlinn D, Minchin PR, O'Hara
789   RB, Simpson GL, Solymos P, Stevens MHH. 2019. vegan: Community Ecology Package. R
790   package version 2.5-6.
791 Palma S. 2008. Zooplankton distribution and abundance in the austral Chilean channels and
792   fjords. In: Silva N, Palma S eds. *Progress in the oceanographic knowledge of Chilean*
793   *interior waters, from Puerto Montt to Cape Horn.* Comité Oceanográfico Nacional -
794   Pontificia Universidad Católica de Valparaíso, Valparaíso, 107–113.
795 Palma S, Apablaza P, Soto D. 2007. Diversity and aggregation areas of planktonic cnidarians of
796   the southern channels of Chile (Boca del Guafo to Pulluche Channel). *Investigaciones*
797   *Marinas* 35:71–82. DOI: 10.4067/S0717-71782007000200008.
798 Palma S, Kaiser K. 1993. *Plancton marino de aguas Chilenas*. Ediciones Universitarias de
799   Valparaíso.
800 Palma S, Rosales SA. 1997. Sifonóforos epipelágicos de los Canales Australes Chilenos (41º 30'
801   - 46º 40' S). *Ciencia y Tecnología del Mar* 20:125–145.
802 Palma S, Silva N. 2004. Distribution of siphonophores, chaetognaths, euphausiids and
803   oceanographic conditions in the fjords and channels of southern Chile. *Deep-Sea Research*
804   *II* 51:513–535. DOI: 10.1016/j.dsr2.2004.05.001.
805 Palma S, Silva N, Retamal MC, Castro L. 2011. Seasonal and vertical distributional patterns of
806   siphonophores and medusae in the Chiloé Interior Sea, Chile. *Continental Shelf Research*
807   31:260–271. DOI: 10.1016/j.csr.2010.04.007.
808 Pan J, Marcoval MA, Bazzini SM, Vallina M V., Marco SG de. 2013. Coastal marine
809   biodiversity challenges and threats. In: Arias AH, Menendez MC eds. *Marine Ecology in a*
810   *Changing World*. CRC Press, 43–67. DOI: 10.1201/b16334-3.
811 Pantoja S, Iriarte JL, Daneri G. 2011. Oceanography of the Chilean Patagonia. *Continental Shelf*
812   *Research* 31:149–153. DOI: 10.1016/j.csr.2010.10.013.
813 Pérez-Santos I, Castro L, Ross L, Niklitschek E, Mayorga N, Cubillos L, Gutierrez M, Escalona
814   E, Castillo M, Alegría N, Daneri G. 2018. Turbulence and hypoxia contribute to dense
815   zooplankton scattering layers in Patagonian Fjord System. *Ocean Science* 14:1185–2018.
816   DOI: 10.5194/os-2017-89.
817 Pérez-Santos I, Garcés-Vargas J, Schneider W, Ross L, Parra S, Valle-Levinson A. 2014.
818   Double-diffusive layering and mixing in Patagonian fjords. *Progress in Oceanography*
819   129:35–49. DOI: 10.1016/j.pocean.2014.03.012.
820 Picheral M, Colin S, Irisson J-O. 2017. EcoTaxa, a tool for the taxonomic classification of
821   images. http://ecotaxa.obs-vlfr.fr.

822   R Core Team. 2021. R: A language and environment for statistical computing.

823   Ramírez B. 1995. Distribución de la biomasa pigmentaria en los Canales Australes. In:
824   *Resúmenes Resultados Crucero Cimar Fiordo 1*. 74–75.

825   Sánchez N, González HE, Iriarte JL. 2011. Trophic interactions of pelagic crustaceans in Comau
826   Fjord (Chile): Their role in the food web structure. *Journal of Plankton Research* 33:1212–
827   1229. DOI: 10.1093/plankt/fbr022.

828   Schneider CA, Rasband WS, Eliceiri KW. 2012. NIH Image to ImageJ: 25 years of image
829   analysis. *Nature Methods* 9:671–675. DOI: 10.1038/nmeth.2089.

830   Sievers HA, Silva N. 2008. Water masses and circulation in austral Chilean channels and fjords.
831   In: Silva N, Palma S eds. *Progress in the oceanographic knowledge of Chilean interior*
832   *waters, from Puerto Montt to Cape Horn.* Comité Oceanográfico Nacional - Pontificia
833   Universidad Católica de Valparaíso, Valparaíso, 53–58.

834   Silva N, Calvete C, Sievers HA. 1997. Características Oceanográficas Físicas y Químicas de
835   Canales Australes Chilenos entre Puerto Montt y Laguna San Rafael (Crucero Cimar-Fiordo
836   1). *Ciencia y Tecnología del Mar* 20:23–106.

837   Stich HB, Lampert W. 1981. Predator evasion as an explanation of diurnal vertical migration by
838   zooplankton. *Nature* 293:396–398. DOI: 10.1038/293396a0.

839   Tutasi P, Escribano R. 2020. Zooplankton diel vertical migration and downward C flux into the
840   oxygen minimum zone in the highly productive upwelling region off Northern Chile.
841   *Biogeosciences* 17:455–473. DOI: 10.5194/bg-2019-127.

842   Urrère MA, Knauer GA. 1981. Zooplankton fecal pellet fluxes and vertical transport of
843   particulate organic material in the pelagic environment. *Journal of Plankton Research*
844   3:369–387. DOI: 10.1093/plankt/3.3.369.

845   Valle-Levinson A, Castro L, Cáceres M, Pizarro O. 2014. Twilight vertical migrations of
846   zooplankton in a Chilean fjord. *Progress in Oceanography* 129:114–124. DOI:
847   10.1016/j.pocean.2014.03.008.

848   Vandromme P, Stemmann L, Garcia-Comas C, Berline L, Sun X, Gorsky G. 2012. Assessing
849   biases in computing size spectra of automatically classified zooplankton from imaging
850   systems: a case study with the ZooScan integrated system. *Methods in Oceanography* 1–
851   2:3–21. DOI: 10.5194/bgd-7-9175-2010.

852   Vargas CA, Martínez RA, González HE, Silva N. 2008. Contrasting trophic interactions of
853   microbial and copepod communities in a fjord ecosystem , Chilean Patagonia. *Aquatic*
854   *Microbial Ecology* 53:227–242. DOI: 10.3354/ame01242.

855   Villenas F, Soto D, Palma S. 2009. Cambios interanuales en la biomasa y biodiversidad de
856   zooplancton gelatinoso en aguas interiores de Chiloé, sur de Chile (primaveras 2004 y
857   2005). *Revista de Biologia Marina y Oceanografia* 44:309–324. DOI: 10.4067/s0718-
858   19572009000200005.

859

Regression coefficients between individual dry mass and body area to estimate biomass

[DM (µg) = (a A^b)] for different groups given by Lehette and Hernández-León (2009). Area provides the size range for each category observed in this study

1 Table 1 Regression coefficients between individual dry mass and body area to estimate biomass
2 [DM (μg) = $(a\ A^b)$] for different groups given by Lehette and Hernández-León (2009). Area
3 provides the size range for each category observed in this study.

Organism	*a*	*b*	*Area (mm²)*
Actinopterygii (eggs and larvae)	43.38	1.54	0.079 – 1.198
Appendicularia	43.38	1.54	0.056 – 6.071
Ascidiacea (larvae)	43.38	1.54	0.072 – 1.652
Amphipoda	43.38	1.54	0.103 – 59.854
Brachiopoda (larvae)	43.38	1.54	0.193 – 0.366
Bivalvia (larvae)	43.38	1.54	0.071 – 2.040
Bryozoa (larvae)	43.38	1.54	0.067 – 0.240
Chaetognatha	23.45	1.19	0.068 – 15.935
Cirripedia (larvae and cypris)	43.38	1.54	0.071 – 0.286
Cladocera	43.38	1.54	0.072 – 0.455
Cnidaria	4.03	1.24	0.051 – 95.743
Copepoda	43.97	1.52	0.068 – 9.177
Decapoda (zoea)	43.38	1.54	0.072 – 6.733
Echinodermata	43.38	1.54	0.070 – 0.757
Euphausiacea	43.38	1.54	0.145 – 461.813
Eggs	43.38	1.54	0.070 – 1.952
Gastropoda (larvae)	43.38	1.54	0.071 – 2.266
Isopoda	43.38	1.54	0.073 – 0.930
Mysidacea	43.38	1.54	0.126 – 43.504
Nemertea (pilidium)	43.38	1.54	0.082 – 0.777
Ostracoda	43.38	1.54	0.066 – 1.270
Platyhelminthes (larvae)	43.38	1.54	0.075 – 0.162
Polychaeta (larvae)	43.38	1.54	0.068 – 7.535

6

Integrated abundances (ind m^{-2}) of the most important zooplankton taxa over the entire water column sampled on four dates throughout a year.

1 Table 2 Integrated abundances (ind m^{-2}) of the most important zooplankton groups over the
2 entire water column sampled on four dates throughout a year.

		SPRING		SUMMER		AUTUMN		WINTER	
		Day	Night	Day	Night	Day	Night	Day	Night
Cyclopoida		47,894	28,198	5,974	6,501	2,227	4,342	3,209	3,477
	Mean	38,046		6,237		3,284		3,343	
Harpacticoida		48,632	47,978	9,664	12,421	9,929	7,486	6,514	4,345
	Mean	48,305		11,042		8,707		5,429	
Copepoda (nauplii)		20,600	18,129	1,481	2,583	431	2,094	2,463	1,616
	Mean	19,365		2,032		1,263		2,039	
Metridinidae		27,772	9,287	25,691	8,105	12,696	18,262	4,438	1,684
	Mean	18,529		16,897		15,479		3,061	
Calanidae		11,288	7,447	5,898	2,827	3,622	3,087	1,977	889
	Mean	9,367		4,363		3,354		1,433	
Euchaetidae		1,840	4,259	1,731	1,110	790	873	1,060	733
	Mean	3,045		1,420		831		896	
Cnidaria		4,895	2,546	1,520	3,713	702	2,432	4,636	2,848
	Mean	3,721		2,616		1,567		3,742	
Chaetognatha		3,108	1,216	2,528	1,187	884	1,390	1,000	598
	Mean	2,162		1,858		1,117		799	
Mysida		239	171	62	164	151	411	239	166
	Mean	205		113		280		202	

Figure 1

Study site.

(A) Overview of Chilean Patagonia. Red square denotes area in panel B. (B) Inner Sea off Chiloé island, where Comau Fjord (red dot) is located. (C) Comau Fjord with the bathymetry and location of the station where zooplankton samples were taken (red dot). Adapted from Fillinger & Richter (2013a).
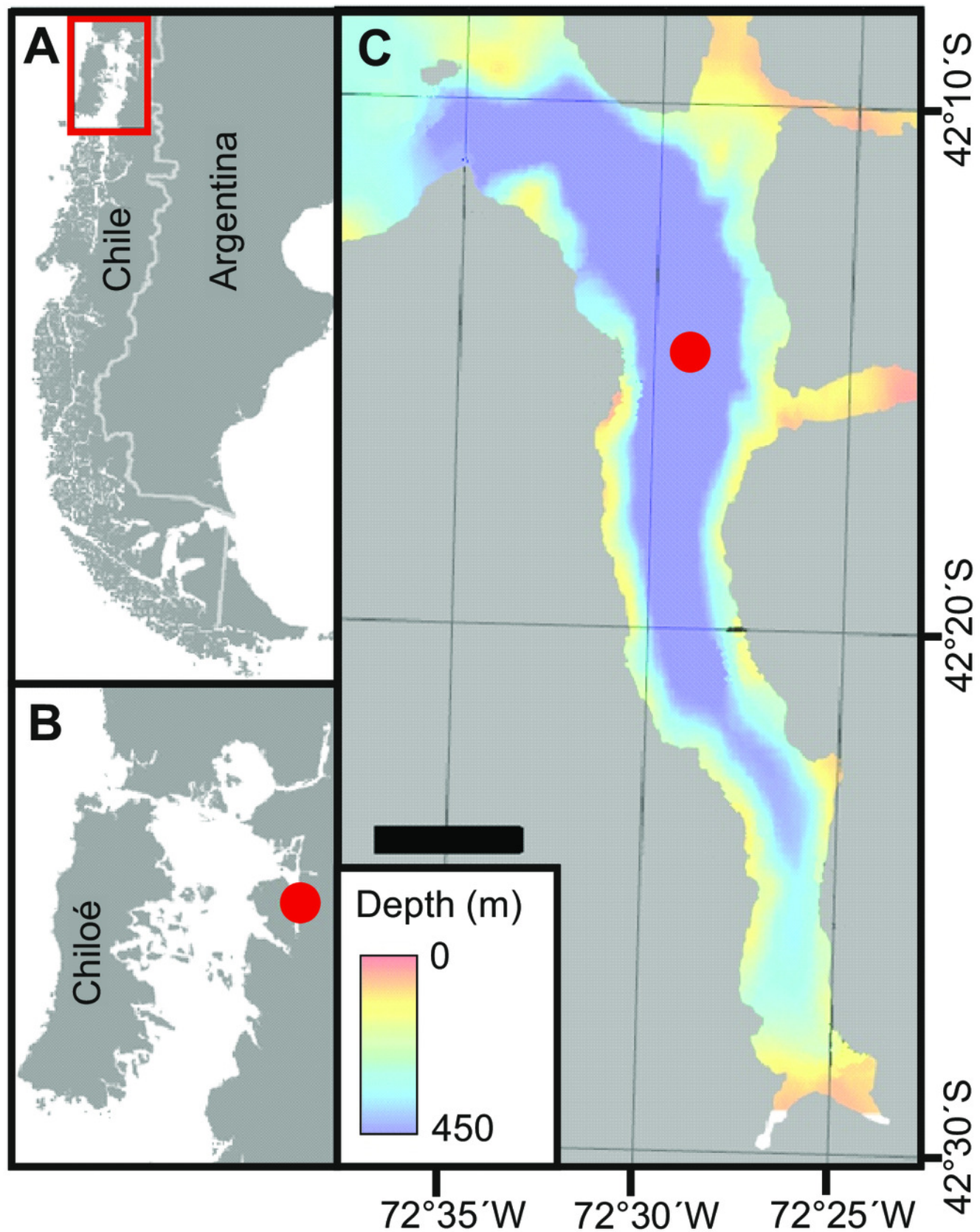
Figure 2

Vertical profiles of physico-chemical parameters of Comau Fjord.

(A) temperature, (B) salinity, (C) pH, (D) oxygen and (E) Chlorophyll-*a*. Note the break at 100 m with the different scales above and below.
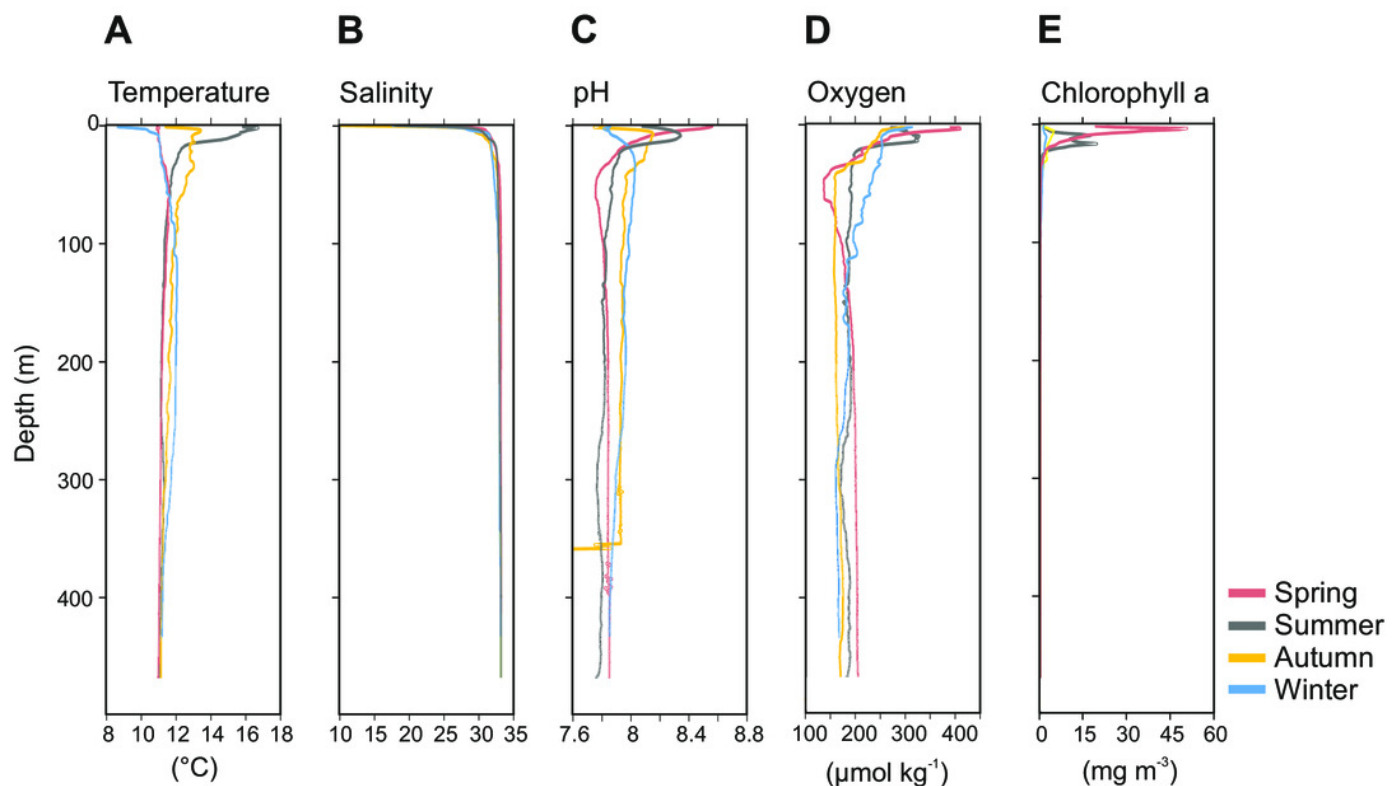
Figure 3

Zooplankton seasonal and diel distribution.

Seasonal distribution of integrated (A) abundance, (B) biovolume and (C) biomass of the zooplankton community during day and night.
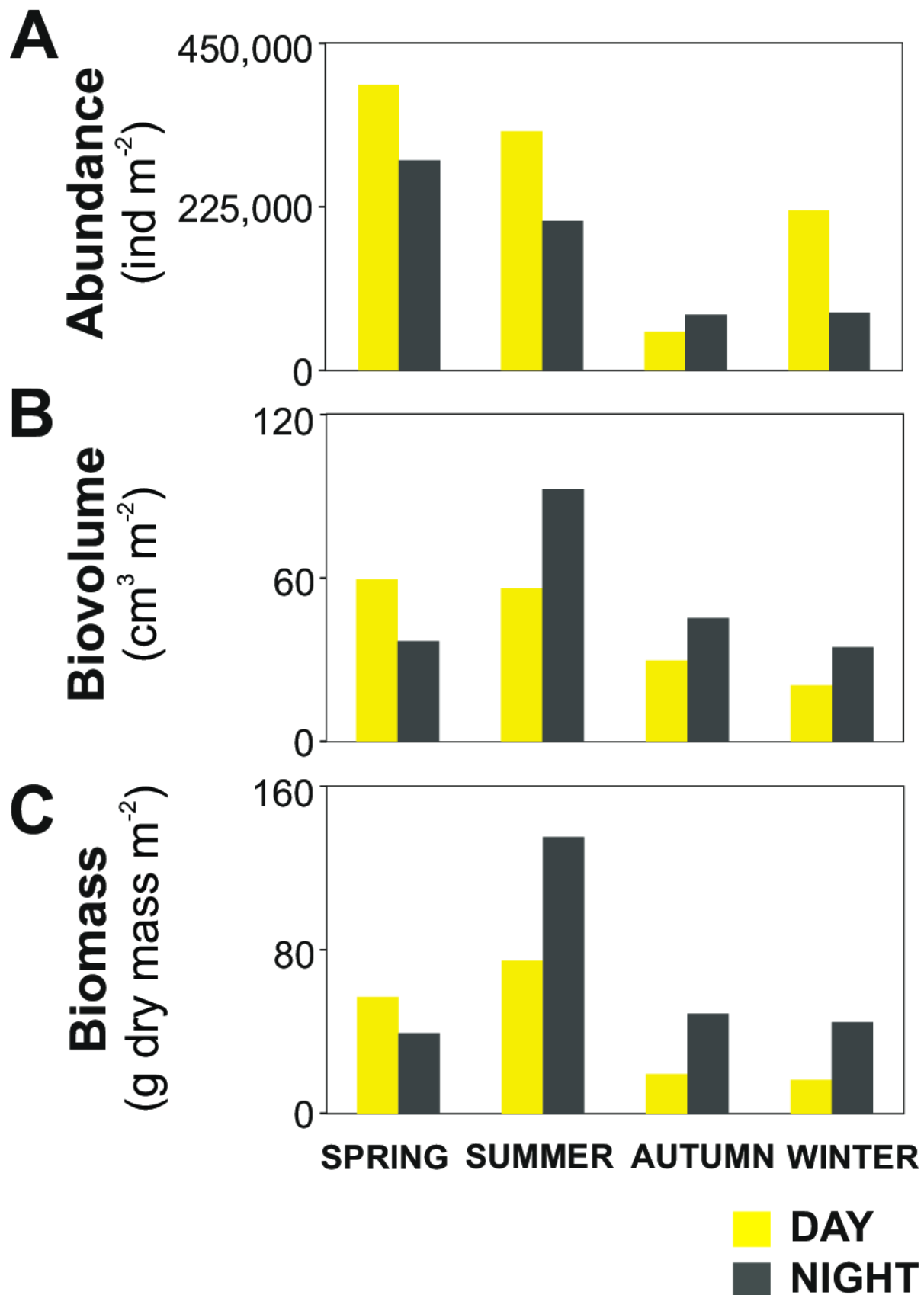
Figure 4

Dissimilarity analysis of day-night differences in centroid depth (CD).

Zooplankton taxa which contribute cumulatively to at least 70% of the day-night differences in (A) abundance CD and (B) biovolume CD.
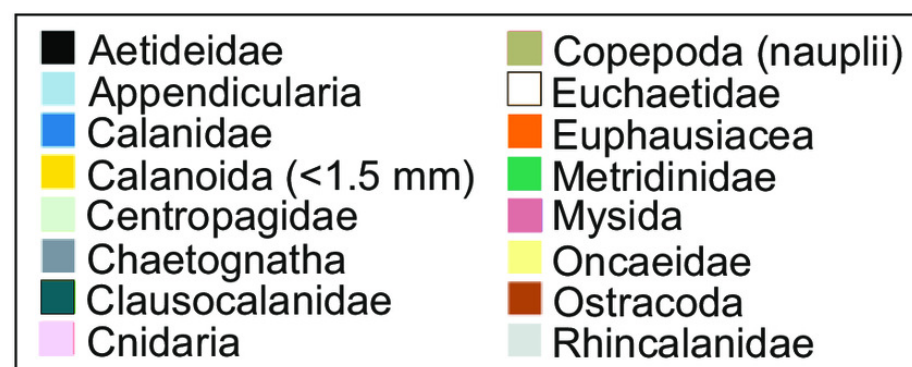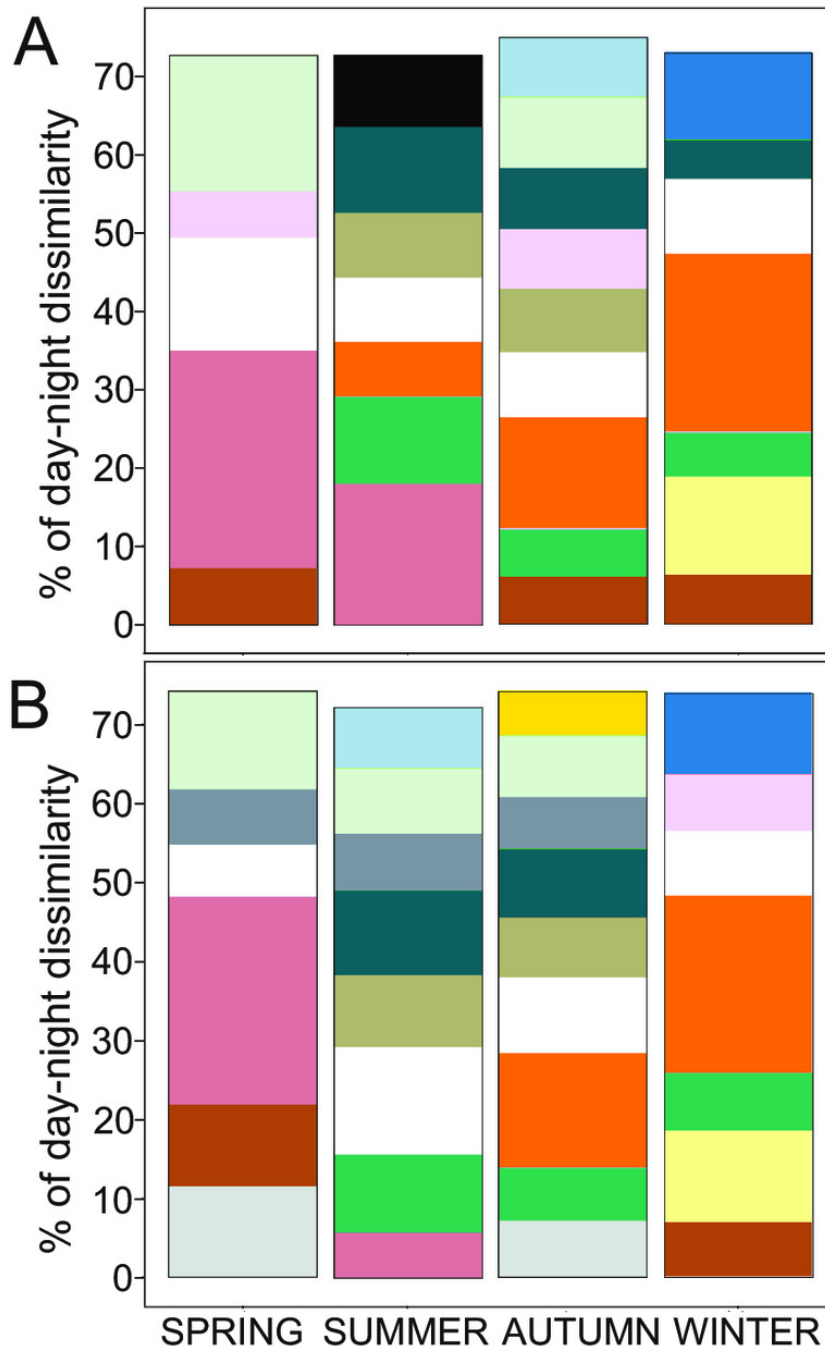
Figure 5

Zooplankton vertical distribution.

Seasonal, diel and vertical distribution of (A) abundance, (B) biovolume and (C) biomass of the zooplankton community during day and night.

Abundance (ind m⁻³)

A

Biovolume (cm³ m⁻³)

B

Biomass (g dry mass m⁻³)

C

SPRING   SUMMER   AUTUMN   WINTER

DAY
NIGHT
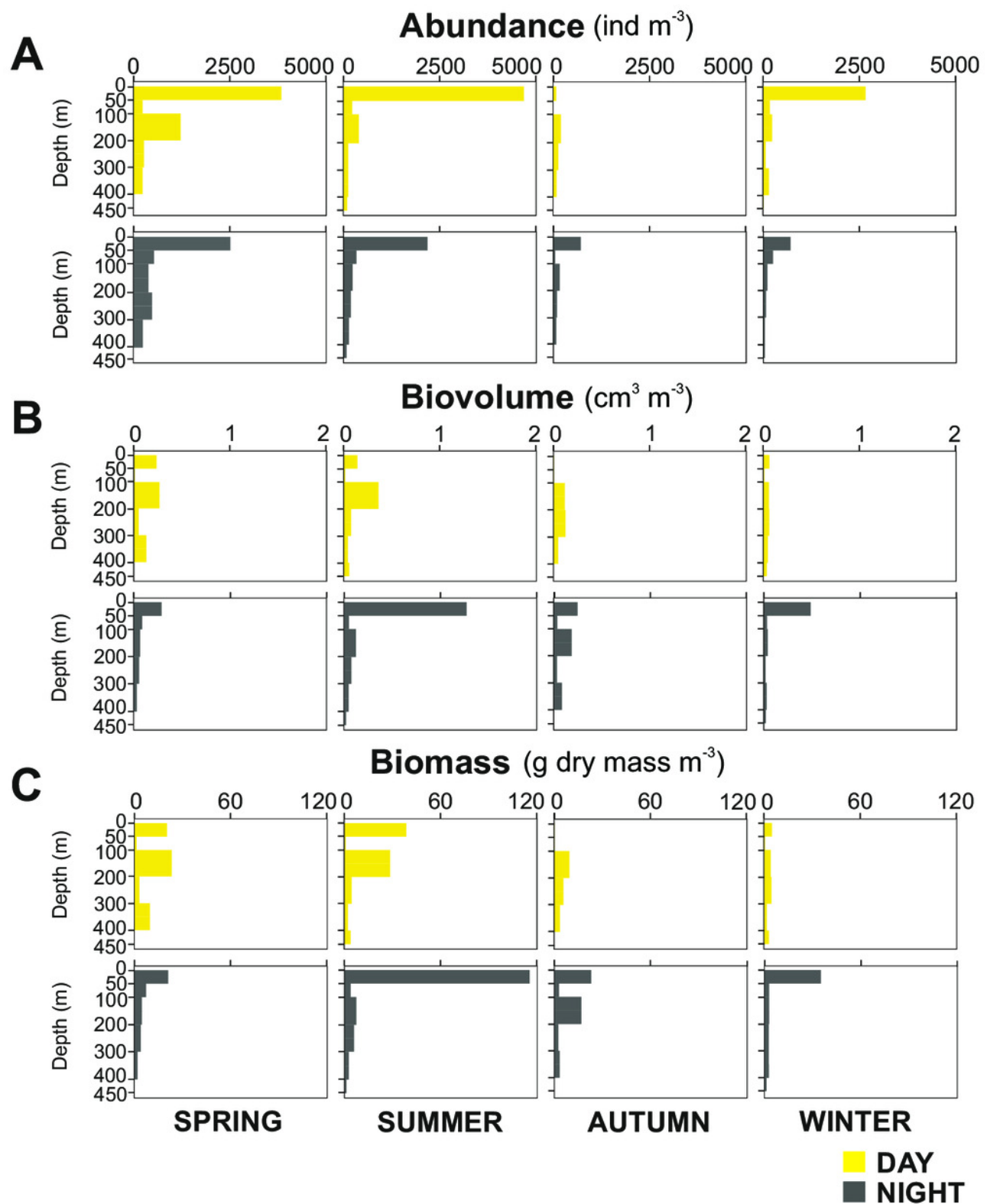
Figure 6

Group dominance of the mesozooplankton taxa.

Relative (A) abundance and (B) biovolume of major zooplankton groups. Taxa comprising less than 3% of the total zooplankton community (27 taxa) were pooled together as "other".
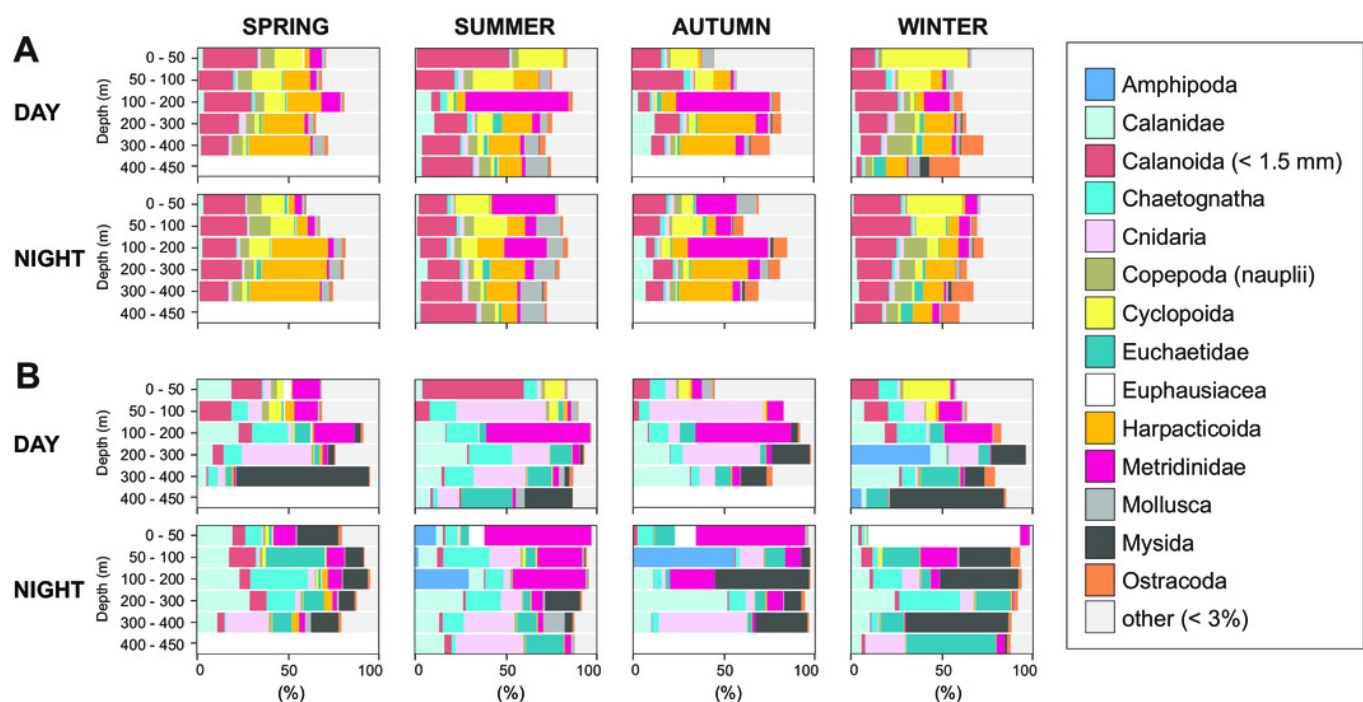
Figure 7

Seasonal, diel and vertical distribution of the most important taxa.

Vertical, diel and seasonal distribution of the most important taxa representing the percent of abundance and biovolume (%) in relation to their total abundance and biovolume. In (A) is presented the total sum of biovolume and abundance in all samples. Vertical distributions of (B) Metridinidae, (C) Calanidae, (D) Harpacticoida, (E) Cnidaria, (F) Mysida, (G) Chaetognatha, (H) Cyclopoida and (I) Euchaetidae. The group "calanoids (<1.5 mm)", although more than 5% in both, biovolume and abundance, is not represented here as it is composed of a mix of taxa with different functions.
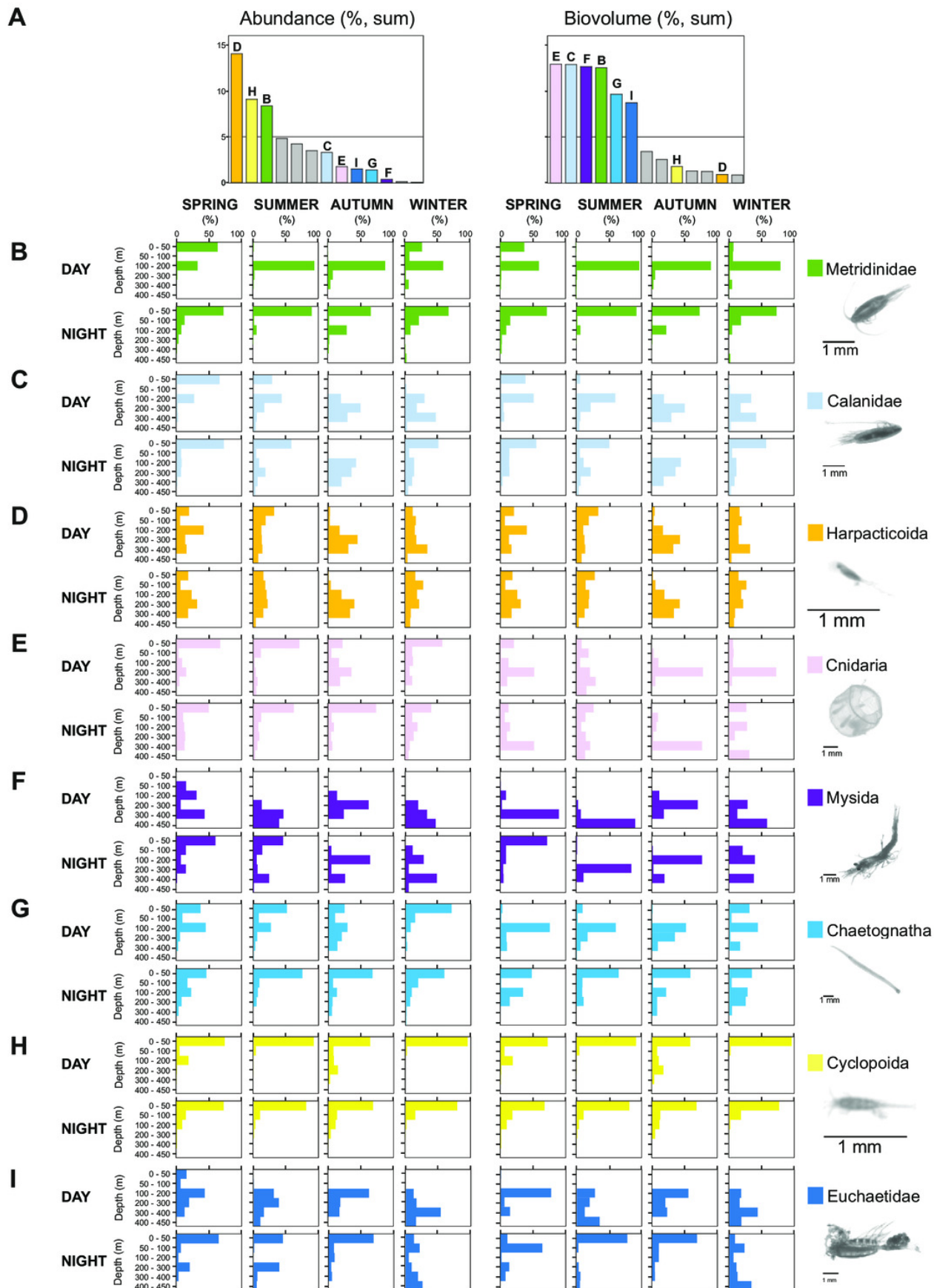
Figure 8

Size frequency distribution of Metridinidae and Calanidae (Copepoda).

Seasonal, diel and vertical size-frequency distribution of (A) Metridinidae and (B) Calanidae. (#) provides the number of individuals measured.

A Metridinidae

B Calanidae

DAY   NIGHT

DAY   NIGHT

SPRING   Depth (m)

0 - 50
50 - 100
100 - 200
200 - 300
300 - 400
400 - 450

SUMMER   Depth (m)

0 - 50
50 - 100
100 - 200
200 - 300
300 - 400
400 - 450

AUTUMN   Depth (m)

0 - 50
50 - 100
100 - 200
200 - 300
300 - 400
400 - 450

WINTER   Depth (m)

0 - 50
50 - 100
100 - 200
200 - 300
300 - 400
400 - 450

mm³   mm³   mm³   mm³
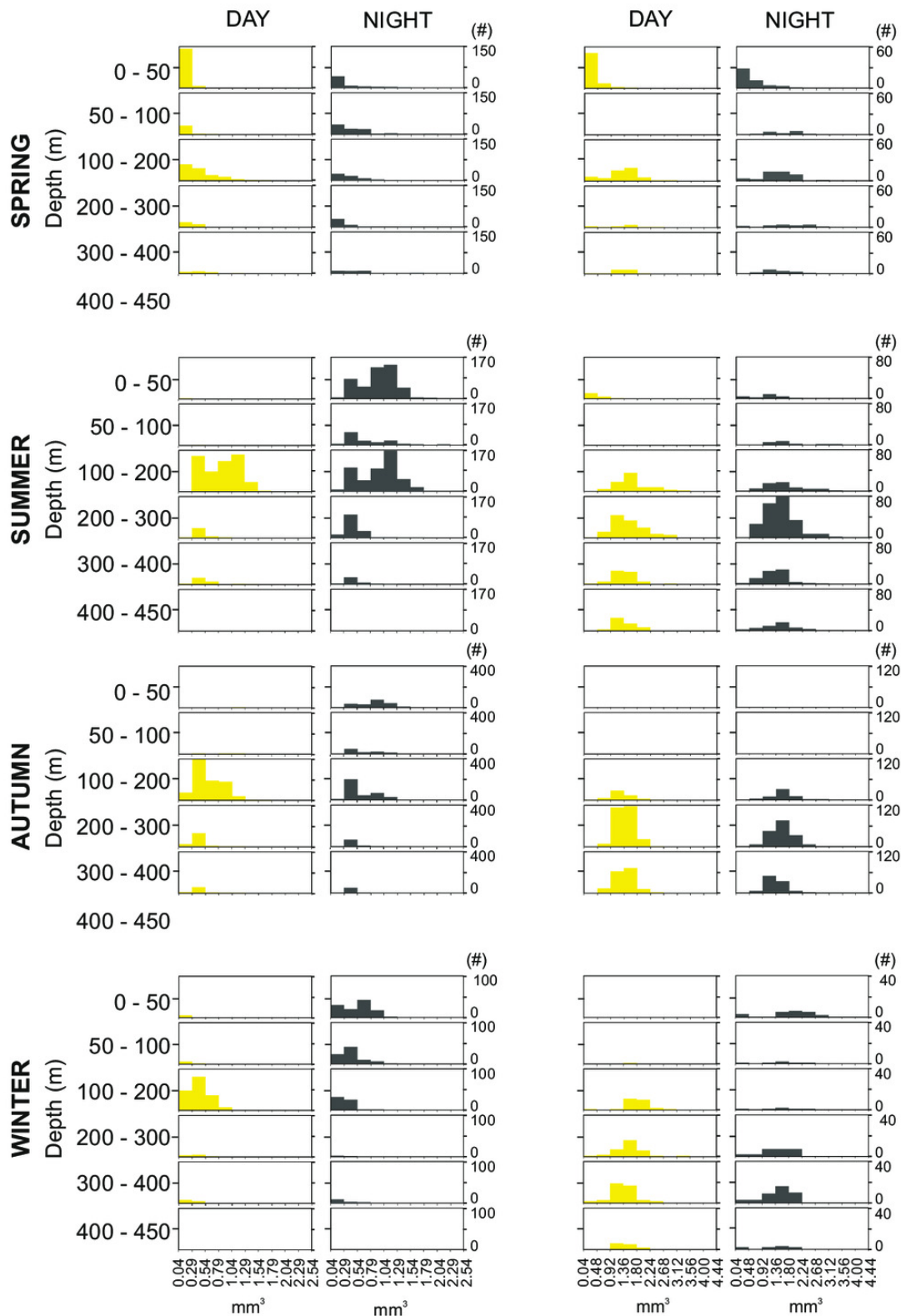
Figure 9

Non-carnivore copepods versus carnivore zooplankton.

Presented as percentages of (A) total abundance and (B) total biovolume.